

Mixed-Variable Bayesian Optimization

Erik Daxberger^{*,†,1,2}, Anastasia Makarova^{*,3}, Matteo Turchetta^{2,3} and Andreas Krause³

¹Department of Engineering, University of Cambridge

²Max Planck Institute for Intelligent Systems, Tübingen

³Department of Computer Science, ETH Zurich

ead54@cam.ac.uk, {anmakaro,matteo.turchetta,krausea}@inf.ethz.ch

Abstract

The optimization of expensive to evaluate, black-box, mixed-variable functions, i.e. functions that have continuous and discrete inputs, is a difficult and yet pervasive problem in science and engineering. In Bayesian optimization (BO), special cases of this problem that consider fully continuous or fully discrete domains have been widely studied. However, few methods exist for mixed-variable domains and none of them can handle discrete constraints that arise in many real-world applications. In this paper, we introduce MiVABO, a novel BO algorithm for the efficient optimization of mixed-variable functions combining a linear surrogate model based on expressive feature representations with Thompson sampling. We propose an effective method to optimize its acquisition function, a challenging problem for mixed-variable domains, making MiVABO the first BO method that can handle complex constraints over the discrete variables. Moreover, we provide the first convergence analysis of a mixed-variable BO algorithm. Finally, we show that MiVABO is significantly more sample efficient than state-of-the-art mixed-variable BO algorithms on several hyperparameter tuning tasks, including the tuning of deep generative models.

1 Introduction

Bayesian optimization (BO) [Moćkus, 1975] is a well-established paradigm to optimize costly-to-evaluate, complex, black-box objectives that has been successfully applied to many scientific domains. Most of the existing BO literature focuses on objectives that have purely *continuous* domains, such as those arising in tuning of continuous hyperparameters of machine learning algorithms, recommender systems, and preference learning [Shahriari *et al.*, 2016]. More recently, problems with purely *discrete* domains, such as food safety control and model-sparsification in multi-component systems [Baptista and Poloczek, 2018] have been considered.

However, many real-world optimization problems in science and engineering are of *mixed-variable* nature, involv-

ing *both* continuous and discrete input variables, and exhibit complex constraints. For example, tuning the hyperparameters of a convolutional neural network involves both continuous variables, e.g., learning rate and momentum, and discrete ones, e.g., kernel size, stride and padding. Also, these hyperparameters impose validity constraints, as some combinations of kernel size, stride and padding define invalid networks. Further examples of mixed-variable, potentially constrained, optimization problems include sensor placement [Krause *et al.*, 2008], drug discovery [Negoescu *et al.*, 2011], optimizer configuration [Hutter *et al.*, 2011] and many others. Nonetheless, only few BO methods can address the unconstrained version of such problem and no existing method can handle the constrained one. This work introduces the first algorithm that can efficiently optimize mixed-variable functions subject to known constraints with provable convergence guarantees.

Related Work. Extending *continuous* BO methods [Shahriari *et al.*, 2016] to mixed inputs requires ad-hoc relaxation methods to map the problem to a fully continuous one and rounding methods to map the solution back. This ignores the original domain structure, makes the solution quality dependent on the relaxation and rounding methods, and makes it hard to handle discrete constraints. Extending *discrete* BO methods [Baptista and Poloczek, 2018; Oh *et al.*, 2019] to mixed inputs requires a discretization of the continuous domain part, the granularity of which is crucial: If it is too small, the domain becomes prohibitively large; if it is too large, the domain may only contain poorly performing values of the continuous inputs. Few BO methods address the mixed-variable setting. SMAC [Hutter *et al.*, 2011] uses a random forest surrogate model. However, its frequentist uncertainty estimates may be too inaccurate to steer the sampling. TPE [Bergstra *et al.*, 2011] uses kernel density estimation to find inputs that will likely improve upon and unlikely perform worse than the incumbent solution. While SMAC and TPE can handle hierarchical constraints, they cannot handle more general constraints over the discrete variables, e.g., cardinality constraints. They also lack convergence guarantees. Hyperband (HB) [Li *et al.*, 2018] uses cheap but less accurate approximations of the objective to dynamically allocate resources for function evaluations. BOHB [Falkner *et al.*, 2018] is the model-based counterpart of HB, based on TPE. They thus extend existing mixed-variable methods to the multi-fidelity setting rather than propos-

*Equal contribution. †Work done while at ETH Zurich.

ing new ones, which is complementary to our approach, rather than in competition with it. [Garrido-Merchán and Hernández-Lobato, 2018] propose a Gaussian process kernel to model discrete inputs without rounding bias. Their method lacks guarantees and cannot handle discrete constraints. We instead use discrete optimizers for the acquisition function, which avoid bias by only making integer evaluations. Finally, while [Hernández-Lobato *et al.*, 2015; Gardner *et al.*, 2014; Sui *et al.*, 2015] extend continuous BO methods to handle unknown constraints, no method can handle known discrete constraints in a mixed-variable domain.

Contributions. We introduce MIVABO, the first BO algorithm for efficiently optimizing mixed-variable functions subject to known linear and quadratic integer constraints, encompassing many of the constraints present in real-world domains (e.g. cardinality, budget and hierarchical constraints). It relies on a linear surrogate model that decouples the continuous, discrete and mixed components of the function using an expressive feature expansion (Sec. 3.1). We exploit the ability of this model to efficiently draw samples from the posterior over the objective (Sec. 3.2) by combining it with Thompson sampling, and show how to optimize the resulting constrained acquisition function (Sec. 3.3). While in continuous BO, optimizing the acquisition function is difficult but has well-established solutions, this is not true for mixed-variable spaces and doing this efficiently and accurately is a key challenge that hugely impacts the algorithm’s performance. We also provide the first convergence analysis of a mixed-variable BO algorithm (Sec. 3.5). Finally, we demonstrate the effectiveness of MIVABO on a set of complex hyperparameter tuning tasks, where it outperforms state-of-the-art methods and is competitive with human experts (Sec. 4).

2 Problem Statement

We consider the problem of optimizing an unknown, costly-to-evaluate function defined over a mixed-variable domain, accessible through noisy evaluations and subject to known linear and quadratic constraints. Formally, we aim to solve

$$\min_{\mathbf{x} \in \mathcal{X}} f(\mathbf{x}) \quad \text{s.t.} \quad g^c(\mathbf{x}) \geq 0, g^d(\mathbf{x}) \geq 0, \quad (1)$$

where $\mathcal{X} \subseteq \mathcal{X}^c \times \mathcal{X}^d$ with continuous subspace \mathcal{X}^c and discrete subspace \mathcal{X}^d . Both constraints $g^c(\mathbf{x}) \geq 0$ over \mathcal{X}^c and $g^d(\mathbf{x}) \geq 0$ over \mathcal{X}^d are known, and specifically $g^d(\mathbf{x})$ are linear or quadratic. We assume, that the domain of the continuous inputs is box-constrained and can thus, w.l.o.g., be scaled to the unit hypercube, $\mathcal{X}^c = [0, 1]^{D_c}$. We further assume, w.l.o.g., that the discrete inputs are binary, i.e., vectors $\mathbf{x}^d \in \mathcal{X}^d = \{0, 1\}^{D_d}$ are vertices of the unit hypercube. This representation can effectively capture the domain of any discrete function. For example, a vector $\mathbf{x}^d = [x_i^d]_{i=1}^{D_d} \in \mathcal{X}^d$ can encode a subset A of a ground set of D_d elements, such that $x_i^d = 1 \Leftrightarrow a_i \in A$ and $x_i^d = 0 \Leftrightarrow a_i \notin A$, yielding a set function. Alternatively, $\mathbf{x}^d \in \mathcal{X}^d$ can be a binary encoding of integer variables, yielding a function defined over integers.

Background. BO algorithms are iterative black-box optimization methods which, at every step t , select an input $\mathbf{x}_t \in \mathcal{X}$ and observe a noise-perturbed output $y_t \triangleq f(\mathbf{x}_t) + \epsilon$ with $\epsilon \stackrel{\text{iid}}{\sim} \mathcal{N}(0, \beta^{-1})$, $\beta > 0$. As evaluating f is costly, the

goal is to query inputs based on past observations to find a global minimizer $\mathbf{x}_* \in \arg \min_{\mathbf{x} \in \mathcal{X}} f(\mathbf{x})$ as efficiently and accurately as possible. To this end, BO algorithms leverage two components: (i) a *probabilistic function model* (or *surrogate*), that encodes the belief about f based on the observations available, and (ii) an *acquisition function* $\alpha : \mathcal{X} \rightarrow \mathbb{R}$ that expresses the informativeness of input \mathbf{x} about the location of \mathbf{x}_* , given the surrogate of f . Based on the model of f , we query the best input measured by the acquisition function, then update the model with the observation and repeat this procedure. The goal of the acquisition function is to simultaneously learn about inputs that are likely to be optimal and about poorly explored regions of the input space, i.e., to trade-off exploitation against exploration. Thus, BO reduces the original hard black-box optimization problem to a series of cheaper problems $\mathbf{x}_t \in \arg \max_{\mathbf{x} \in \mathcal{X}} \alpha_t(\mathbf{x})$. However, in our case, these optimization problems involve mixed variables and exhibit linear and quadratic constraints and are thus still challenging. We now present MIVABO, an algorithm to efficiently solve the optimization problem in Eq. (1).

3 MIVABO Algorithm

We first introduce the linear model used to represent the objective (Sec. 3.1) and describe how to do inference with it (Sec. 3.2). We then show how to use Thompson sampling to query informative inputs (Sec. 3.3) and, finally, provide a bound on the regret incurred by MIVABO. (Sec. 3.5).

3.1 Model

We propose a surrogate model that accounts for both discrete and continuous variables in a principled way, while balancing two conflicting goals: Model expressiveness versus feasibility of Bayesian inference and of the constrained optimization of the mixed-variable acquisition function. Linear models defined over non-linear feature mappings, $f(\mathbf{x}) = \mathbf{w}^\top \phi(\mathbf{x})$, are a class of flexible parametric models that strike a good trade-off between model capacity, interpretability and ease of use through the definition of features $\phi : \mathcal{X} \rightarrow \mathbb{R}^M$. While the complexity of the model is controlled by the number of features, M , its capacity depends on their definition. Therefore, to make the design of a set of expressive features more intuitive, we treat separately the contribution to the objective f from the discrete part of the domain, from the continuous part of the domain, and from the interaction of the two,

$$f(\mathbf{x}) = \sum_{j \in \{d, c, m\}} \mathbf{w}^j \phi^j(\mathbf{x}^j) \quad (2)$$

where, for $j \in \{d, c, m\}$, $\phi^j(\mathbf{x}^j) = [\phi_i^j(\mathbf{x}^j)]_{i=1}^{M_j} \in \mathbb{R}^{M_j}$ and $\mathbf{w}^j \in \mathbb{R}^{M_j}$ are the feature and weight vector for the discrete, continuous and mixed function component, respectively.

In many real-world domains, a large set of features can be discarded *a priori* to simplify the design space. It is common practice in high-dimensional BO to assume that only low-order interactions between the variables contribute significantly to the objective, which was shown for many practical problems [Rolland *et al.*, 2018; Mutný and Krause, 2018], including deep neural network hyperparameter tuning [Hazan *et al.*, 2017]. Similarly, we focus on features defined over small subsets of the inputs. Formally, we consider

$\phi(\mathbf{x}) = [\phi_k(\mathbf{x}_k)]_{k=1}^M$, where \mathbf{x}_k is a subvector of \mathbf{x} containing exclusively continuous or discrete variables or a mix of both. Thus, the objective $f(\mathbf{x})$ can be decomposed into a sum of low-dimensional functions $f_k(\mathbf{x}_k) \triangleq w_k \phi_k(\mathbf{x}_k)$ defined over subspaces $\mathcal{X}_k \subseteq \mathcal{X}$ with $\dim(\mathcal{X}_k) \ll \dim(\mathcal{X})$. This defines a *generalized additive model* [Rolland *et al.*, 2018; Hastie, 2017], where the same variable can be included in multiple subvectors/features. The complexity of this model is controlled by the *effective dimensionality* (ED) of the subspaces, which is crucial under limited computational resources. In particular, let $\bar{D}_d \triangleq \max_{k \in [M]} \dim(\mathcal{X}_k^d)$ denote the ED of the discrete component in Eq. (2), i.e. the dimensionality of the largest subspace that exclusively contains discrete variables. Analogously, \bar{D}_c and \bar{D}_m denote the EDs of the continuous and mixed component, respectively. Intuitively, the ED corresponds to the maximum order of the variable interactions present in f . Then, the number of features $M \in \mathcal{O}(D_d^{\bar{D}_d} + D_c^{\bar{D}_c} + (D_d + D_c)^{\bar{D}_m})$ scales exponentially in the EDs only (as modeling up to L -th order interactions of N inputs requires $\sum_{l=0}^L \binom{N}{l} \in \mathcal{O}(N^L)$ terms), which are usually small, even if the true dimensionality is large.

Discrete Features ϕ^d . We aim to define features ϕ^d that can effectively represent the discrete component of Eq. (2) as a linear function, which should generally be able to capture arbitrary interactions between the discrete variables. To this end, we consider all subsets S of the discrete variables in \mathcal{X}^d (or, equivalently, all elements S of the powerset $2^{\mathcal{X}^d}$ of \mathcal{X}^d) and define a monomial $\prod_{j \in S} x_j^d$ for each subset S (where for $S = \emptyset$, $\prod_{j \in \emptyset} x_j^d = 1$). We then form a weighted sum of all monomials to yield the multi-linear polynomial $\mathbf{w}^{d\top} \phi^d(\mathbf{x}^d) = \sum_{S \in 2^{\mathcal{X}^d}} w_S \prod_{j \in S} x_j^d$. This functional representation corresponds to the Fourier expansion of a *pseudo-Boolean function* (PBF) [Boros and Hammer, 2002]. In practice, an exponential number of features can be prohibitively expensive and may lead to high-variance estimators as in BO one typically does not have access to enough data to robustly fit a large model. Alternatively, [Baptista and Poloczek, 2018; Hazan *et al.*, 2017] empirically found that a second-order polynomial in the Fourier basis provides a practical balance between expressiveness and efficiency, even when the true function is of higher order. In our model, we also consider quadratic PBFs, $\mathbf{w}^{d\top} \phi^d(\mathbf{x}^d) = w_\emptyset + \sum_{i=1}^n w_{\{i\}} x_i^d + \sum_{1 \leq i < j \leq n} w_{\{i,j\}} x_i^d x_j^d$, which induces the discrete feature representation $\phi^d(\mathbf{x}^d) \triangleq [1, \{x_i^d\}_{i=1}^{D_d}, \{x_i^d x_j^d\}_{1 \leq i < j \leq D_d}]^\top$ and reduces the number of model weights to $M_d \in \mathcal{O}(D_d^2)$.

Continuous Features ϕ^c . In BO over continuous spaces, most approaches are based on Gaussian process (GP) models [Williams and Rasmussen, 2006] due to their flexibility and ability to capture large classes of continuous functions. To fit our linear model formulation, we leverage GPs' expressiveness by modeling the continuous part of our model in Eq. (2) using feature expansions $\phi^c(\mathbf{x}^c)$ that result in a finite linear approximation of a GP. One simple, yet theoretically sound, choice is the class of Random Fourier Features (RFFs) [Rahimi and Recht, 2008], which use Monte Carlo integration for a randomized approximation of a GP. Alternatively,

one can use Quadrature Fourier Features [Mutný and Krause, 2018], which instead use numerical integration for a deterministic approximation, which is particularly effective for problems with low effective dimensionality. Both feature classes were successfully used in BO [Janatton *et al.*, 2017; Mutný and Krause, 2018]. In our experiments, we use RFFs approximating a GP with a squared exponential kernel, which we found to best trade off complexity vs. accuracy in practice.

Mixed Features ϕ^m . The mixed term should capture as rich and realistic interactions between the discrete and continuous variables as possible, while keeping model inference and acquisition function optimization efficient. To this end, we stack products of all pairwise combinations of features of the two variable types, i.e. $\phi^m(\mathbf{x}^d, \mathbf{x}^c) \triangleq [\phi_i^d(\mathbf{x}^d) \cdot \phi_j^c(\mathbf{x}^c)]_{1 \leq i \leq M_d, 1 \leq j \leq M_c}^\top$. This formulation provides a good trade-off between modeling accuracy and computational complexity. In particular, it allows us to reduce ϕ^m to the discrete feature representation ϕ^d when conditioned on a fixed assignment of continuous variables ϕ^c (and vice versa). This property is crucial for optimizing the acquisition function, as it allows us to optimize the mixed term of our model by leveraging the tools for optimizing the discrete and continuous parts individually. The proposed representation contains $M_d M_c$ features, resulting in a total of $M = M_d + M_c + M_d M_c$. To reduce model complexity, prior knowledge about the problem can be incorporated into the construction of the mixed features. In particular, one may consider the following approaches. Firstly, one can exploit a known interaction structure between variables, e.g., in form of a dependency graph, and ignore the features that are known to be irrelevant. Secondly, one can start by including all of the proposed pairwise feature combinations and progressively discard not-promising ones. Finally, for high-dimensional problems, one can do the opposite and progressively add pairwise feature combinations, starting from the empty set.

3.2 Model Inference

Let $\mathbf{X}_{1:t} \in \mathbb{R}^{t \times D}$ be the matrix whose i^{th} row contains the input $\mathbf{x}_i \in \mathcal{X}$ queried at iteration i , $\dim \mathcal{X} = D$, and let $\mathbf{y}_{1:t} = [y_1, \dots, y_t]^\top \in \mathbb{R}^t$ be the array of the corresponding noisy function observations. Also, let $\Phi_{1:t} \in \mathbb{R}^{t \times M}$ be the matrix whose i^{th} row contains the featurized input $\phi(\mathbf{x}_i) \in \mathbb{R}^M$. The formulation of f in Eq. (2) and the noisy observation model induce the Gaussian likelihood $p(\mathbf{y}_{1:t} | \mathbf{X}_{1:t}, \mathbf{w}) = \mathcal{N}(\Phi_{1:t} \mathbf{w}, \beta^{-1} \mathbf{I})$. To reflect our *a priori* belief about the weight vector \mathbf{w} and thus f , we specify a prior distribution over \mathbf{w} . A natural choice for this is a zero-mean isotropic Gaussian prior $p(\mathbf{w} | \alpha) = \mathcal{N}(\mathbf{0}, \alpha^{-1} \mathbf{I})$, with precision $\alpha > 0$, which encourages \mathbf{w} to be uniformly small, so that the final predictor is a sum of all features, each giving a small, non-zero contribution. Given the likelihood and prior, we infer the posterior $p(\mathbf{w} | \mathbf{X}_{1:t}, \mathbf{y}_{1:t}, \alpha, \beta) \propto p(\mathbf{y}_{1:t} | \mathbf{X}_{1:t}, \mathbf{w}, \beta) p(\mathbf{w} | \alpha)$, which due to conjugacy is Gaussian, $p(\mathbf{w} | \mathbf{X}_{1:t}, \mathbf{y}_{1:t}) = \mathcal{N}(\mathbf{m}, \mathbf{S}^{-1})$, with mean $\mathbf{m} = \beta \mathbf{S}^{-1} \Phi_{1:t}^\top \mathbf{y}_{1:t} \in \mathbb{R}^M$ and precision $\mathbf{S} = \alpha \mathbf{I} + \beta \Phi_{1:t}^\top \Phi_{1:t} \in \mathbb{R}^{M \times M}$ [Williams and Rasmussen, 2006]. This simple analytical treatment of the posterior distribution over \mathbf{w} is a main benefit of this model, which can be viewed as a GP with a linear kernel in feature space.

3.3 Acquisition Function

We propose to use Thompson sampling (TS) [Thompson, 1933], which samples weights $\tilde{\mathbf{w}} \sim p(\mathbf{w}|\mathbf{X}_{1:t}, \mathbf{y}_{1:t}, \alpha, \beta)$ from the posterior and chooses the next input by solving $\hat{\mathbf{x}} \in \arg \min_{\mathbf{x} \in \mathcal{X}} \tilde{\mathbf{w}}^\top \phi(\mathbf{x})$. TS intuitively focuses on inputs that are plausibly optimal and has previously been successfully applied in both discrete and continuous domains [Baptista and Poloczek, 2018; Mutný and Krause, 2018].

TS requires solving $\hat{\mathbf{x}} \in \arg \min_{\mathbf{x} \in \mathcal{X}} \tilde{\mathbf{w}}^\top \phi(\mathbf{x})$, which is a challenging mixed-variable optimization problem. However, as $\tilde{\mathbf{w}}^\top \phi(\mathbf{x})$ decomposes as in Eq. (2), we can naturally use an alternating optimization scheme which iterates between optimizing the discrete variables \mathbf{x}^d conditioned on a particular setting of the continuous variables \mathbf{x}^c and vice versa, until convergence to some local optimum. While this scheme provides no theoretical guarantees, it is simple and thus widely and effectively applied in many contexts where the objective is hard to optimize. In particular, we iteratively solve $\hat{\mathbf{x}}^d \in \arg \min_{\mathbf{x}^d \in \mathcal{X}^d} (\tilde{\mathbf{w}}^{d\top} \phi^d(\mathbf{x}^d) + \tilde{\mathbf{w}}^{m\top} \phi^m(\mathbf{x}^d, \mathbf{x}^c = \hat{\mathbf{x}}^c))$, $\hat{\mathbf{x}}^c \in \arg \min_{\mathbf{x}^c \in \mathcal{X}^c} (\tilde{\mathbf{w}}^{c\top} \phi^c(\mathbf{x}^c) + \tilde{\mathbf{w}}^{m\top} \phi^m(\mathbf{x}^d = \hat{\mathbf{x}}^d, \mathbf{x}^c))$. Importantly, using the mixed features proposed in Sec. 3.1, these problems can be optimized by purely discrete and continuous optimizers, respectively. This also holds in the presence of mixed constraints $g^m(\mathbf{x}) \geq 0$ if those decompose accordingly into discrete and continuous constraints.

This scheme leverages independent subroutines for discrete and continuous optimization: For the discrete part, we exploit the fact that optimizing a second-order pseudo-Boolean function is equivalent to a binary integer quadratic program (IQP) [Boros and Hammer, 2002], allowing us to exploit commonly-used efficient and robust solvers such as Gurobi or CPLEX. While solving general binary IQPs is NP-hard [Boros and Hammer, 2002], these optimizers are in practice very efficient for the dimensionalities we consider (i.e., $D_d < 100$). This approach allows us to use any functionality offered by these tools, such as the ability to optimize objectives subject to linear constraints $\mathbf{A}\mathbf{x}^d \leq \mathbf{b}$, $\mathbf{A} \in \mathbb{R}^{K \times D_d}$, $\mathbf{b} \in \mathbb{R}^K$ or quadratic constraints $\mathbf{x}^{d\top} \mathbf{Q}\mathbf{x}^d + \mathbf{q}^\top \mathbf{x}^d \leq b$, $\mathbf{Q} \in \mathbb{R}^{D_d \times D_d}$, $\mathbf{q} \in \mathbb{R}^{D_d}$, $b \in \mathbb{R}$. For the continuous part, one can use optimizers commonly used in continuous BO, such as L-BFGS or DIRECT. In our experiments, we use Gurobi as the discrete and L-BFGS as the continuous solver within the alternating optimization scheme, which we always run until convergence.

3.4 Model Discussion

BO algorithms are comprised of three major design choices: the surrogate model to estimate the objective, the acquisition function to measure informativeness of the inputs and the acquisition function optimizer to select queries. Due to the widespread availability of general-purpose optimizers for continuous functions, continuous BO is mostly concerned with the first two design dimensions. However, this is different for mixed-variable constrained problems. We show in Sec. 4 that using a heuristic optimizer for the acquisition function optimization leads to poor queries and, therefore, poor performance of the BO algorithm. Therefore, the tractability of the acquisition function optimization influences

and couples the other design dimensions. In particular, the following considerations make the choice of a linear model and TS the ideal combination of surrogate and acquisition function for our problem. Firstly, the linear model is preferable to a GP with a mixed-variable kernel as the latter would complicate the acquisition function optimization for two reasons: (i) the posterior samples would be arbitrary nonlinear functions of the discrete variables and (ii) it would be non-trivial to evaluate them at arbitrary points in the domain. In contrast, our explicit feature expansion solves both problems, while second order interactions provide a valid discrete function representation [Baptista and Poloczek, 2018; Hazan *et al.*, 2017] and lead to tractable quadratic MIPs with capacity for complex discrete constraints. Moreover, Random Fourier Features approximate common GP kernels arbitrarily well, and inference in MiVABO scales linearly with the number of data points, making it applicable in cases where GP inference, which scales cubically with the number of data points, would be prohibitive. Secondly, TS induces a simple relation between the surrogate and the resulting optimization problem for the acquisition function, allowing to trade off model expressiveness and optimization tractability, which is a key challenge in mixed-variable domains. Finally, the combination of TS and the linear surrogate facilitates the convergence analysis described in Sec. 3.5, making MiVABO the first mixed-variable BO method with theoretical guarantees.

3.5 Convergence Analysis

Using a linear model and Thompson sampling, we can leverage convergence analysis from linearly parameterized multi-armed bandits, a well-studied class of methods for solving structured decision making problems [Abeille *et al.*, 2017]. These also assume the objective to be linear in features $\phi(\mathbf{x}) \in \mathbb{R}^M$ with a fixed but unknown weight vector $\mathbf{w} \in \mathbb{R}^M$, i.e. $\mathbb{E}[f(\mathbf{x})|\phi(\mathbf{x})] = \mathbf{w}^\top \phi(\mathbf{x})$, and aim to minimize the *total regret* up to time T : $\mathcal{R}(T) = \sum_{t=1}^T (f(\mathbf{x}_*) - f(\mathbf{x}_t))$. We obtain the following regret bound for MiVABO:

Proposition 1. *Assume that the following assumptions hold in every iteration $t = 1, \dots, T$ of the MiVABO algorithm:*

1. $\tilde{\mathbf{w}}_t \sim \mathcal{N}(\mathbf{m}, 24M \ln T \ln \frac{1}{\delta} \mathbf{S}^{-1})$, i.e. with scaled variance.
2. $\mathbf{x}_t = \arg \min_{\mathbf{x}} \tilde{\mathbf{w}}^\top \phi(\mathbf{x})$ is selected exactly.¹
3. $\|\tilde{\mathbf{w}}_t\|_2 \leq c$, $\|\phi(\mathbf{x}_t)\|_2 \leq c$, $\|f(\mathbf{x}_*) - f(\mathbf{x}_t)\|_2 \leq c$, $c \in \mathbb{R}^+$.

Then, $\mathcal{R}(T) \leq \tilde{O}\left(M^{3/2} \sqrt{T} \ln \frac{1}{\delta}\right)$ with probability $1 - \delta$.

Prop. 1 follows from Theorem 1 in [Abeille *et al.*, 2017] and works for infinite arms $\mathbf{x} \in \mathcal{X}$, $|\mathcal{X}| = \infty$. In our setting, both the discrete and continuous Fourier features (and, thus, the mixed features) satisfy the standard boundedness assumption, such that the proof indeed holds. Prop. 1 implies *no-regret*, $\lim_{T \rightarrow \infty} \mathcal{R}(T)/T = 0$, i.e., convergence to the global minimum, since the minimum found after T iterations is no further away from $f(\mathbf{x}_*)$ than the mean regret $\mathcal{R}(T)/T$. To our knowledge, MiVABO is the first mixed-variable BO algorithm for which such a guarantee is known to hold.

¹To this end, one can use more expensive but theoretically backed optimization methods instead of the alternating one, such as the powerful and popular *dual decomposition* [Sontag *et al.*, 2011].

4 Experiments

We present experimental results on tuning the hyperparameters of two machine learning algorithms, namely gradient boosting and a deep generative model, on multiple datasets.

Experimental Setup. For MIVABO², we set the prior variance α , observation noise variance β , and kernel bandwidth σ to 1.0, and scale the variance as stated in Prop. 1. We compare against SMAC, TPE, random search, and the popular GPyOpt BO package. GPyOpt uses a GP model with the upper confidence bound acquisition function [Srinivas *et al.*, 2010], and accounts for mixed variables by relaxing discrete variables to be continuous and later rounding them to the nearest discrete neighbor. To separate the influence of model choice and acquisition function optimization, we also consider the MIVABO model optimized by simulated annealing (SA) (MIVABO-SA) and the GP approach optimized by SA (GP-SA). We compare against the SA-based variants only in constrained settings, using more principled methods in unconstrained ones. To handle constraints, SA assigns high energy values to invalid inputs, making the probability of moving there negligible. We use SMAC, TPE and GPyOpt and SA with their respective default settings.

4.1 Gradient Boosting Tuning

The OpenML database [Vanschoren *et al.*, 2014] contains evaluations for various machine learning methods trained on several datasets with many hyperparameter settings. We consider extreme gradient boosting (XGBoost) [Chen and Guestrin, 2016], one of the most popular OpenML benchmarks, and tune its ten hyperparameters – three are discrete and seven continuous – to minimize the classification error on a held-out test set (without any constraints). We use two datasets, each containing more than 45000 hyperparameter settings. To evaluate hyperparameter settings for which no data is available, we use a surrogate modeling approach based on nearest neighbor [Eggenberger *et al.*, 2015], meaning that the objective returns the error of the closest (w.r.t. Euclidean distance) setting available in the dataset. Fig. 1 shows that MIVABO achieves performance which is either significantly stronger than (left dataset) or competitive with (right dataset) the state-of-the-art mixed-variable BO algorithms on this challenging task. GPyOpt performs poorly, likely because it cannot account for discrete variables in a principled way. As compared to TPE and SMAC, MIVABO seems to benefit from more sophisticated uncertainty estimation.

4.2 Deep Generative Model (DGM) Tuning

DGMs recently received considerable attention in the machine learning community. Despite their popularity and importance, effectively tuning their hyperparameters is a major challenge. We consider tuning the hyperparameters of a variational autoencoder (VAE) [Kingma and Welling, 2014] composed of a convolutional encoder and a deconvolutional decoder [Salimans *et al.*, 2015]. The VAEs are evaluated on stochastically binarized MNIST, as in [Burda *et al.*, 2016],

and FashionMNIST. They are trained on 60000 images for 32 epochs, using Adam with a mini-batch size of 128. We report the negative log-likelihood (NLL; in nats) achieved by the VAEs on a held-out test set of 10000 images, as estimated via importance sampling using 32 samples per test point. To our knowledge, no other BO paper considered DGM tuning.

VAE tuning is difficult due to the high-dimensional and structured nature of its hyperparameter space, and, in particular, due to constraints arising from dependencies between some of its parameters. We tune 25 discrete parameters defining the model architecture, e.g. the number of convolutional layers, their stride, padding and filter size, the number and width of fully-connected layers, and the latent space dimensionality. We further tune three continuous parameters for the optimizer and regularization. Crucially, mutual dependencies between the discrete parameters result in complex constraints, as certain combinations of stride, padding and filter size lead to invalid architectures. Particularly, for the encoder, the shapes of all layers must be integral, and for the decoder, the output shape must match the input data shape, i.e., one channel of size 28×28 for {Fashion}MNIST. The latter constraint is especially challenging, as only a small number of decoder configurations yield the required output shape. Thus, even for rather simple datasets such as {Fashion}MNIST, tuning such a VAE is significantly more challenging than, say, tuning a convolutional neural network for classification.

While MIVABO can conveniently capture these restrictions via linear and quadratic constraints, the competing methods cannot. To enable a comparison that is as fair as possible, we thus use the following sensible heuristic to incorporate the knowledge about the constraints into the baselines: If a method tries to evaluate an invalid parameter configuration, we return a penalty error value, which will discourage a model-based method to sample this (or a similar) setting again. However, for fairness, we only report valid observations and ignore all configurations that violated a constraint. We set the penalty value to 500 nats, which is the error incurred by a uniformly random generator. We investigated the impact of the penalty value (e.g., we also tried 250 and 125 nats) and found that it does *not* qualitatively affect the results.

Fig. 3 shows that MIVABO significantly outperforms the competing methods on this task, both on MNIST (left) and FashionMNIST (right). This is because MIVABO can naturally encode the constraints and thus directly optimize over the feasible region in parameter space, while TPE, SMAC and GPyOpt need to learn the constraints from data. They fail to do so and get stuck in bad local optima early on. The model-based approaches likely struggle due to sharp discontinuities in hyperparameter space induced by the constraint violation penalties (i.e., as invalid configurations may lie close to well-performing configurations). In contrast, random search is agnostic to these discontinuities, and thus notably outperforms the model-based methods. Lastly, GP-SA and MIVABO-SA struggle as well, suggesting that while SA can avoid invalid inputs, the effective optimization of complex constrained objectives crucially requires more principled approaches for acquisition function optimization, such as the one we propose. This shows that all model choices for MIVABO (as discussed in Sec. 3.4) are necessary to achieve such strong results.

²We provide a Python implementation of MIVABO at https://github.com/edaxberger/mixed_variable_bo.

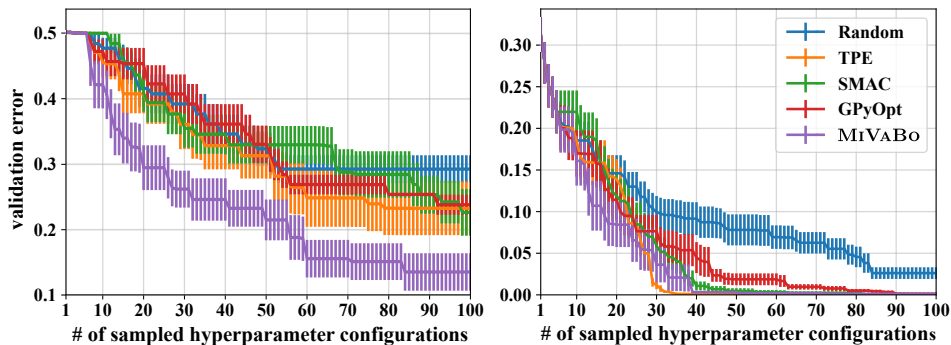


Figure 1: **XGBoost hyperparameter tuning** on `monks-problem-1` (left) and `steel-plates-fault` (right). Mean \pm one std. of the validation error over 16 random seeds. MiVABO significantly outperforms the baselines on the first dataset, and is competitive on the second.

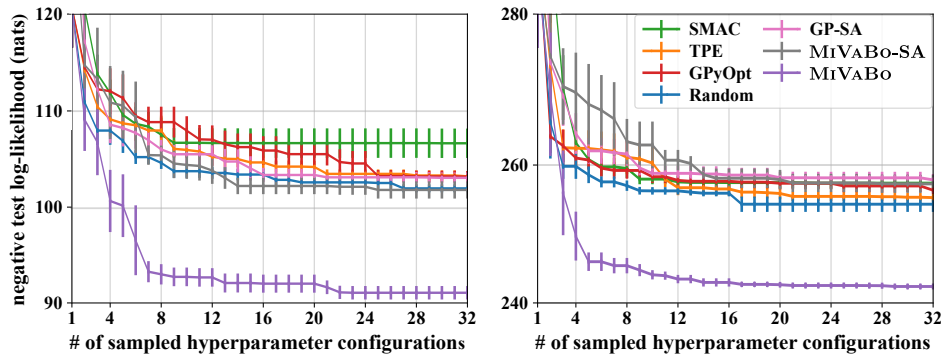


Figure 3: **VAE hyperparameter tuning** on MNIST (left) and FashionMNIST (right). Mean \pm one std. of the NLL in nats, estimated using 32 importance samples, over 8 random seeds. Every model was trained for 32 epochs. MiVABO significantly outperforms the state-of-the-art baselines, demonstrating its ability to handle the complex constrained nature of the VAE’s parameter space.

Although log-likelihood scores allow for a quantitative comparison, they are hard to interpret for humans. Thus, for a qualitative comparison, Fig. 2 visualizes the reconstruction quality achieved on MNIST by the best VAE configuration found by all methods after 32 BO iterations. The VAEs were trained for 32 epochs each, as in Fig. 3. The likelihoods seem to correlate with the quality of appearance, and the model found by MiVABO arguably produces the visually most appealing reconstructions among all models. Note that while MiVABO requires more time than the baselines (see Fig. 4), this is still negligible compared to the cost of a function evaluation, which involves training a deep generative model. Finally, the best VAE found by MiVABO achieves 84.25 nats on MNIST when trained for 3280 epochs and using 5000 importance samples for log-likelihood estimation, i.e. the setting used in [Burda *et al.*, 2016] (see Fig. 4). This is comparable to the performance of 82-83 nats achieved by human expert tuned models, e.g. as reported in [Salimans *et al.*, 2015] (which use even more convolutional layers and a more sophisticated inference method), highlighting MiVABO’s effectiveness in tuning complex deep neural network architectures.

5 Conclusion

We propose MiVABO, the first method for efficiently optimizing expensive mixed-variable black-box functions subject

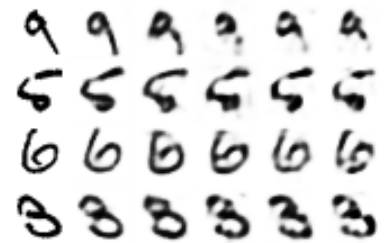


Figure 2: Randomly chosen MNIST test images (left column) and their reconstructions by the best VAE models found by MiVABO, random search, GPyOpt, TPE and SMAC (left to right), thus ordered by NLL values, which seem to capture visual quality.

Method	Time	NLL
SMAC	0.32s	99.09
TPE	0.12s	97.05
GPyOpt	0.65s	97.33
Random	0.01s	93.74
MiVABO	7.39s	84.25

Figure 4: Mean wall-clock time of one iteration (excluding function evaluation time) and mean negative log-likelihood (NLL) in nats, estimated with 5000 importance samples, of the best VAEs found after 32 BO iterations (as in Fig. 3), when trained for 3280 epochs. Human expert baseline for even deeper models is 82-83 nats.

to linear and quadratic discrete constraints. MiVABO combines a linear model of expressive features with Thompson sampling, making it simple yet effective. Moreover, it is highly flexible due to the modularity of its components, i.e., the mixed-variable features, and the optimization oracles for the acquisition procedure. This allows practitioners to tailor MiVABO to specific objectives, e.g. by incorporating prior knowledge in the feature design or by leveraging optimizers handling specific types of constraints. We show that MiVABO enjoys theoretical convergence guarantees that competing methods lack. Finally, we empirically demonstrate that MiVABO significantly improves optimization performance as compared to state-of-the-art methods for mixed-variable optimization on complex hyperparameter tuning tasks.

Acknowledgements

This research has been partially supported by SNSF NFP75 grant 407540.167189. Matteo Turchetta was supported through the ETH-MPI Center for Learning Systems. Erik Daxberger was supported through the EPSRC and Qualcomm. The authors thank Josip Djolonga, Mojmír Mutný, Johannes Kirschner, Alonso Marco Valle, David R. Burt, Ross Clarke, Wolfgang Roth as well as the anonymous reviewers of an earlier version of this paper for their helpful feedback.

References

- [Abeille *et al.*, 2017] Marc Abeille, Alessandro Lazaric, et al. Linear Thompson sampling revisited. *EJS*, 2017.
- [Baptista and Poloczek, 2018] Ricardo Baptista and Matthias Poloczek. Bayesian optimization of combinatorial structures. In *ICML*, 2018.
- [Bergstra *et al.*, 2011] James S Bergstra, Rémi Bardenet, Yoshua Bengio, and Balázs Kégl. Algorithms for hyperparameter optimization. In *NIPS*, 2011.
- [Boros and Hammer, 2002] Endre Boros and Peter L Hammer. Pseudo-boolean optimization. *Discrete applied mathematics*, 123(1-3):155–225, 2002.
- [Burda *et al.*, 2016] Yuri Burda, Roger Grosse, and Ruslan Salakhutdinov. Importance weighted autoencoders. In *ICLR*, 2016.
- [Chen and Guestrin, 2016] Tianqi Chen and Carlos Guestrin. XGBoost: A scalable tree boosting system. In *KDD*, 2016.
- [Eggenberger *et al.*, 2015] Katharina Eggenberger, Frank Hutter, Holger H Hoos, and Kevin Leyton-Brown. Efficient benchmarking of hyperparameter optimizers via surrogates. In *AAAI*, 2015.
- [Falkner *et al.*, 2018] Stefan Falkner, Aaron Klein, and Frank Hutter. BOHB: Robust and efficient hyperparameter optimization at scale. In *ICML*, 2018.
- [Gardner *et al.*, 2014] Jacob R. Gardner, Matt J. Kusner, Zhixiang Xu, Kilian Q. Weinberger, and John P. Cunningham. Bayesian optimization with inequality constraints. In *ICML*, 2014.
- [Garrido-Merchán and Hernández-Lobato, 2018] Eduardo C Garrido-Merchán and Daniel Hernández-Lobato. Dealing with categorical and integer-valued variables in bayesian optimization with gaussian processes. *CoRR*, 2018.
- [Hastie, 2017] Trevor J Hastie. Generalized additive models. In *Statistical models in S*. Routledge, 2017.
- [Hazan *et al.*, 2017] Elad Hazan, Adam Klivans, and Yang Yuan. Hyperparameter optimization: A spectral approach. In *ICRL*, 2017.
- [Hernández-Lobato *et al.*, 2015] José Miguel Hernández-Lobato, Michael A Gelbart, Matthew W Hoffman, Ryan P Adams, and Zoubin Ghahramani. Predictive entropy search for bayesian optimization with unknown constraints. *JMLR*, 2015.
- [Hutter *et al.*, 2011] Frank Hutter, Holger H Hoos, and Kevin Leyton-Brown. Sequential model-based optimization for general algorithm configuration. In *LION*, 2011.
- [Jenatton *et al.*, 2017] Rodolphe Jenatton, Cedric Archambeau, Javier González, and Matthias Seeger. Bayesian optimization with tree-structured dependencies. In *ICML*, 2017.
- [Kingma and Welling, 2014] Diederik P Kingma and Max Welling. Auto-encoding variational bayes. In *ICLR*, 2014.
- [Krause *et al.*, 2008] Andreas Krause, Ajit Singh, and Carlos Guestrin. Near-optimal sensor placements in Gaussian processes: Theory, efficient algorithms and empirical studies. *JMLR*, 2008.
- [Li *et al.*, 2018] Lisha Li, Kevin Jamieson, Giulia DeSalvo, Afshin Rostamizadeh, and Ameet Talwalkar. Hyperband: A novel bandit-based approach to hyperparameter optimization. *JMLR*, 2018.
- [Moćkus, 1975] Jonas Moćkus. On Bayesian methods for seeking the extremum. In *Optimization Techniques*, 1975.
- [Mutný and Krause, 2018] Mojmir Mutný and Andreas Krause. Efficient high dimensional bayesian optimization with additivity and quadrature fourier features. In *NIPS*, 2018.
- [Negoescu *et al.*, 2011] Diana M Negoescu, Peter I Frazier, and Warren B Powell. The knowledge-gradient algorithm for sequencing experiments in drug discovery. *INFORMS*, 2011.
- [Oh *et al.*, 2019] Changyong Oh, Jakub M. Tomczak, Efstratios Gavves, and Max Welling. Combinatorial bayesian optimization using graph representations. *NeurIPS*, 2019.
- [Rahimi and Recht, 2008] Ali Rahimi and Benjamin Recht. Random features for large-scale kernel machines. In *NIPS*, 2008.
- [Rolland *et al.*, 2018] Paul Rolland, Jonathan Scarlett, Ilija Bogunovic, and Volkan Cevher. High-dimensional Bayesian optimization via additive models with overlapping groups. In *AISTATS*, 2018.
- [Salimans *et al.*, 2015] Tim Salimans, Diederik P Kingma, and Max Welling. Markov chain monte carlo and variational inference: Bridging the gap. In *ICML*, 2015.
- [Shahriari *et al.*, 2016] Bobak Shahriari, Kevin Swersky, Ziyu Wang, Ryan P. Adams, and Nando de Freitas. Taking the human out of the loop: A review of Bayesian optimization. *IEEE*, 2016.
- [Sontag *et al.*, 2011] David Sontag, Amir Globerson, and Tommi Jaakkola. Introduction to dual composition for inference. In *Optimization for Machine Learning*. 2011.
- [Srinivas *et al.*, 2010] Niranjan Srinivas, Andreas Krause, Sham M Kakade, and Matthias Seeger. Gaussian process optimization in the bandit setting: No regret and experimental design. In *ICML*, 2010.
- [Sui *et al.*, 2015] Yanan Sui, Alkis Gotovos, Joel Burdick, and Andreas Krause. Safe exploration for optimization with gaussian processes. In *ICML*, 2015.
- [Thompson, 1933] William R Thompson. On the likelihood that one unknown probability exceeds another in view of the evidence of two samples. *Biometrika*, 1933.
- [Vanschoren *et al.*, 2014] Joaquin Vanschoren, Jan N Van Rijn, Bernd Bischl, and Luis Torgo. OpenML: networked science in machine learning. *ACM SIGKDD*, 15(2):49–60, 2014.
- [Williams and Rasmussen, 2006] Christopher KI Williams and Carl Edward Rasmussen. *Gaussian processes for machine learning*. MIT Press Cambridge, MA, 2006.

A Sparse Linear Model via Sparsity-Encouraging Prior

While the number and degree of the features used in the surrogate model (see Section 3.1) is a design choice, in practice it is typically unknown which variable interactions matter and thus which features to choose. To discard irrelevant features, one may impose a sparsity-encouraging prior over the weight vector \mathbf{w} [Baptista and Poloczek, 2018]. However, due to non-conjugacy to the Gaussian likelihood, exact Bayesian inference of the resulting posterior distribution is in general intractable, imposing the need for approximate inference methods. One choice for such a prior is the Laplace distribution, i.e. $p(\mathbf{w}|\alpha) \propto \exp(-\alpha^{-1}\|\mathbf{w}\|_1)$, with inverse scale parameter $\alpha > 0$, for which approximate inference techniques based on expectation propagation [Minka, 2001] and variational inference [Wainwright *et al.*, 2008] were developed in [Seeger, 2008; Seeger and Nickisch, 2008; 2011]. Alternatively, one can use a horseshoe prior and use Gibbs sampling to sample from the posterior over weights [Baptista and Poloczek, 2018]. However, this comes with a significantly larger computational burden, which is a well-known issue for sampling based inference techniques [Bishop, 2006]. Lastly, one may consider a spike-and-slab prior with expectation propagation for approximate posterior inference [Hernández-Lobato *et al.*, 2013; 2015b].

B Pseudocode for Thompson Sampling

Algorithm 1 shows pseudocode for the Thompson sampling procedure within MIVABO.

Algorithm 1 THOMPSON SAMPLING

Require: model features $\phi(\mathbf{x})$

- 1: Set $\mathbf{S} = \mathbf{I}$, $\mathbf{m} = \mathbf{0}$
 - 2: **for** $t = 1, 2, \dots, T$ **do**
 - 3: Sample $\tilde{\mathbf{w}}_t \sim \mathcal{N}(\mathbf{m}, \mathbf{S}^{-1})$
 - 4: Select input $\tilde{\mathbf{x}}_t \in \arg \min_{\mathbf{x} \in \mathcal{X}} \tilde{\mathbf{w}}_t^\top \phi(\mathbf{x})$
 - 5: Query output $y_t = f(\tilde{\mathbf{x}}_t) + \epsilon$
 - 6: Update \mathbf{S} , \mathbf{m} as described in Section 3.2.
 - 7: **end for**
 - 8: **Output:** $\hat{\mathbf{x}}_* \in \arg \min_{\mathbf{x} \in \mathcal{X}} \mathbf{m}^\top \phi(\mathbf{x})$
-

C Further Experimental Results

C.1 Synthetic Benchmark for Unconstrained Optimization

We assess the performance on an unconstrained synthetic linear benchmark function of the form $f(\mathbf{x}) = \mathbf{w}^\top \phi$. We choose a fairly high-dimensional objective with $D_d = 8$ discrete and $D_c = 8$ continuous variables, thus resulting in a total input space dimensionality of $D = D_d + D_c = 16$. For the discrete model part, we choose the $M_d \in \mathcal{O}(D_d^2)$ features ϕ^d proposed in Section 3.1. For the continuous features ϕ^c , we choose $M_c = 16$ dimensional Random Fourier Features to approximate a GP with a squared exponential kernel with

bandwidth $\sigma = 1.0$. For the mixed representation, we construct a feature vector ϕ^m by stacking all pairs of discrete and continuous features, as proposed in Section 3.1. We consider two settings for the weight vector: Firstly, we sample it from a zero-mean Gaussian, $\mathbf{w} \sim \mathcal{N}(\mathbf{0}, \mathbf{I}) \in \mathbb{R}^M$. Secondly, we sample it from a Laplace distribution, i.e. $\mathbf{w} \sim p(\mathbf{w}|\alpha) \propto \exp(-\alpha^{-1}\|\mathbf{w}\|_1)$, with inverse scale parameter $\alpha = 0.1$, and then prune all weights smaller than 10 to zero to induce sparsity over the weight vector. For the second setting, we also assess MIVABO using a Laplace prior and the approximate inference technique from [Seeger and Nickisch, 2011] (see also Appendix A)³. As we do not know the true optimum of the function and thus cannot compute the regret, we normalize all observed function values to the interval $[0, 1]$, resulting in a normalized error as the metric of comparison. We can observe from our results shown in Fig. 5 that MIVABO outperforms the competing methods in this setting, demonstrating the effectiveness of our approach when its modeling assumptions are fulfilled.

C.2 Synthetic Benchmark for Constrained Optimization

In another experiment, we demonstrate the capability of our algorithm to incorporate linear constraints on the discrete variables. In particular, we want to enforce a solution that is sparse in the discrete variables via adding a hard cardinality constraint of the type $\sum_{i=1}^{D_d} x_i^d \leq k$, which we can simply specify in the Gurobi optimizer. Cardinality constraints of this type are very relevant in practice, as many real-world problems desire sparse solutions (e.g., sparsification of ising models, contamination control, aero-structural multi-component problems [Baptista and Poloczek, 2018]). We consider the same functional form as before, i.e. again with $D_d = D_c = 8$, and set $k = 2$, meaning that a solution should have at most two of our binary variables set to one, while all others shall be set to zero. To enable comparison with TPE, SMAC and random search, which provide no capability of modeling these kinds of constraints, we assume the objective f to be unconstrained, but instead return a large penalty value if a method acquires an evaluation of f at a point that violates the constraint. Thus, the baseline algorithms are forced to learn the constraint from observations, which is a challenging problem.

One can notice from Fig. 6 that the ability to explicitly encode the cardinality constraint into the discrete optimization oracle significantly increases performance.

D More Details on XGBoost Hyperparameter Tuning Task

Please refer to the corresponding websites for details on the OpenML XGBoost benchmark (<https://www.openml.org/f/6767>), on the underlying implementation (<https://www.rdocumentation.org/packages/xgboost/versions/0.6-4>), and on the steel-plates-fault (<https://www.openml.org/t/9967>) and monks-problem-1

³We use the MATLAB implementation provided in the `glm-ie` toolbox [Nickisch, 2012] by the same authors.

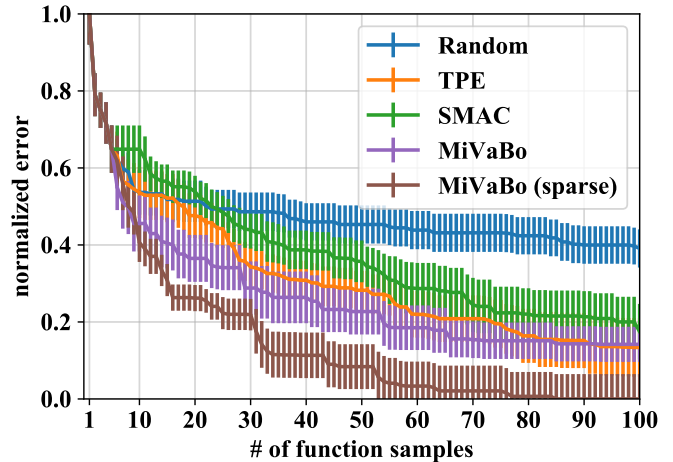
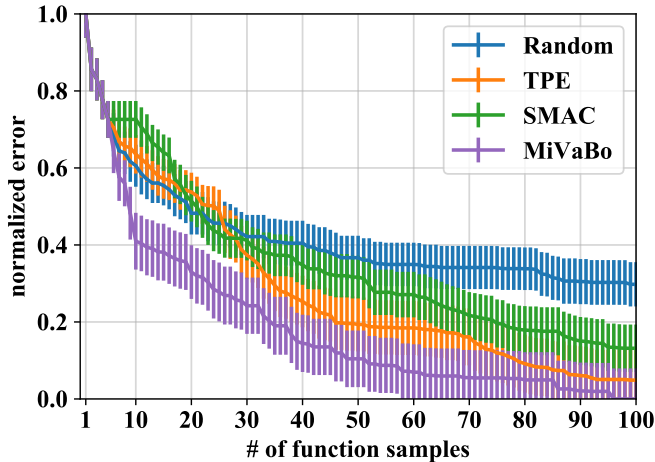


Figure 5: Results on the synthetic benchmark, with the Gaussian (left) and Laplace prior (right). Mean plus/minus one standard deviation of the normalized error over 16 random initializations. (Left) MiVaBo outperforms its competitors. (Right) MiVaBo with a sparse prior outperforms its competitors, including MiVaBo with a Gaussian prior

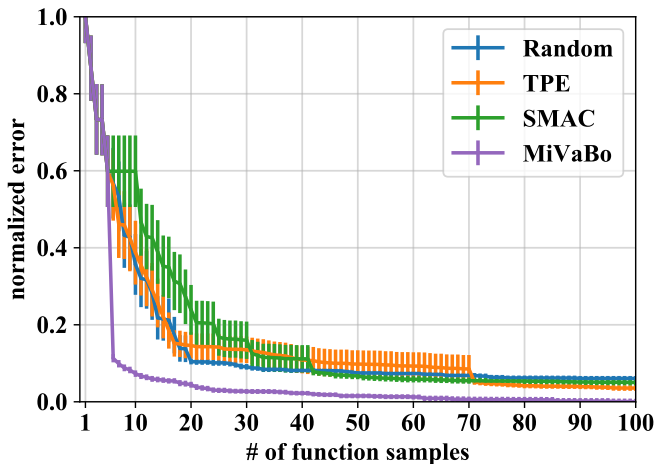


Figure 6: Results on the synthetic benchmark with cardinality constraints. The curves represent the mean plus/minus one standard deviation of the normalized error over 16 random initializations. One can observe that MiVaBo outperforms its competitors.

(<https://www.openml.org/t/146064>) datasets. Finally, see Table 1 for a description of the hyperparameters involved in XGBoost.

E More Details on VAE Hyperparameter Tuning Task

E.1 Hyperparameters of VAE

We used the `PyTorch` library to implement the VAE used in the experiment. Table 2 describes the names, types and domains of the involved hyperparameters that we tune. Whenever we refer to a “deconvolutional layer” (also called transposed convolution or fractionally-strided convolution), we mean the functional mapping implemented by a

Table 1: Hyperparameters of the XGBoost algorithm. 10 parameters, 7 of which are continuous, and 3 of which are discrete.

Name	Type	Domain
booster	discr.	['gbtree', 'gblinear']
nrounds	discr.	[3, 5000]
alpha	contin.	[0.000985, 1009.209690]
lambda	contin.	[0.000978, 999.020893]
colsample_bylevel	contin.	[0.046776, 0.998424]
colsample_bytree	contin.	[0.062528, 0.999640]
eta	contin.	[0.000979, 0.995686]
max_depth	discr.	[1, 15]
min_child_weight	contin.	[1.012169, 127.041806]
subsample	contin.	[0.100215, 0.999830]

`ConvTranspose2d` layer in `PyTorch`⁴. Since our approach operates on a binary encoding of the discrete parameters, we also display the number of bits required to encode each discrete parameter. In total, we consider 25 discrete parameters (resulting in 50 when binarized) as well as three continuous ones.

E.2 Description of Constraints

We now describe the constraints arising from the mutual dependencies within the hyperparameter space of the deconvolutional VAE (as described in Appendix E.1).

Encoder constraints. For the convolutional layers (up to two in our case) of the encoder, we need to ensure that the chosen combination of stride, padding and filter size transforms the input image into an output image whose shape is integral (i.e., not fractional). More precisely, denoting the input image size by W_{in} (i.e., the input image is quadratic with shape $W_{in} \times W_{in}$), the stride by S , the filter size by F , and the

⁴See <https://pytorch.org/docs/stable/nn.html#convtranspose2d> for details.

Table 2: **Hyperparameters of the VAE.** The architecture of the VAE (if all layers are enabled) is C1-C2-F1-F2-z-F3-F4-D1-D2, with C denoting a convolutional (conv.) layer, F a fully-connected (fc.) layer, D a deconvolutional (deconv.) layer and z the latent space. Layers F2 and F3 have fixed sizes of $2d_z$ and d_z units respectively, where d_z denotes the dimensionality of the latent space z. The domain of the number of units of the fc. layers F1 and F4 is discretized with a step size of 64, i.e. $[0, 64, 128, \dots, 832, 896, 960]$, denoted by $[0 \dots 960]$ in the table for brevity. For d_z , the domain $[16 \dots 64]$ refers to all integers within that interval.

#	Name	Type	Domain	Bits
1	Number of conv. layers in encoder	discrete	[0,1,2]	2
	Parameters of C1			
2	Number of channels of C1	discrete	[4,8,16,24]	2
3	Stride of C1	discrete	[1,2]	1
4	Filter size of C1	discrete	[3,5]	1
5	Padding of C1	discrete	[0,1,2,3]	2
	Parameters of C2			
6	Number of channels of C2	discrete	[8,16,32,48]	2
7	Stride of C2	discrete	[1,2]	1
8	Filter size of C2	discrete	[3,5]	1
9	Padding of C2	discrete	[0,1,2,3]	2
10	Number of fc. layers in encoder	discrete	[0,1,2]	2
11	Number of units of F1	discrete	[0...960]	4
12	Dimensionality d_z of z	discrete	[16...64]	6
13	Number of fc. layers in decoder	discrete	[0,1,2]	2
14	Number of units of F4	discrete	[0...960]	4
15	Number of deconv. layers in decoder	discrete	[0,1,2]	2
	Parameters of D1			
16	Number of channels of D1	discrete	[8,16,32,48]	2
17	Stride of D1	discrete	[1,2]	1
18	Filter size of D1	discrete	[3,5]	1
19	Padding of D1	discrete	[0,1,2,3]	2
20	Output padding of D1	discrete	[0,1,2,3]	2
	Parameters of D2			
21	Number of channels of D2	discrete	[4,8,16,24]	2
22	Stride of D2	discrete	[1,2]	1
23	Filter size of D2	discrete	[3,5]	1
24	Padding of D2	discrete	[0,1,2,3]	2
25	Output padding of D2	discrete	[0,1,2,3]	2
26	Learning rate	continuous	$[10^{-4}, 10^{-2}]$	-
27	Learning rate decay factor	continuous	[0.5, 1.0]	-
28	Weight decay regularization	continuous	$[10^{-6}, 10^{-2}]$	-
	Total			50

padding by P , we need to ensure that the output image size W_{out} is integral, i.e.

$$W_{\text{out}}^e = (W_{\text{in}}^e - F^e + P^e)/S^e + 1 \in \mathbb{N} \quad (3)$$

where superscripts e are used to make clear that we are considering the encoder. Let us illustrate this with an example⁵: For $W_{\text{in}} = 10$, $P = 0$, $S = 2$ and $F = 3$, we would get an invalid fractional output size of $W_{\text{out}} = (10 - 3 + 0)/2 + 1 = 4.5$. To obtain a valid output size, one could, e.g., instead

⁵This example is taken from <http://cs231n.github.io/convolutional-networks/#conv> (paragraph "Constraints on strides"), which also describes the constraints discussed here. Note that they define the padding P in a slightly different way (i.e., they only consider symmetric padding, while we also allow for asymmetric padding) and thus end up with a term of $2P$ instead of P in the formula.

consider a padding of $P = 1$, yielding $W_{\text{out}} = (10 - 3 + 1)/2 + 1 = 5$. Alternatively, one could also consider a stride of $S = 1$ to obtain $W_{\text{out}} = (10 - 3 + 0)/1 + 1 = 8$, or a filter size of $F = 4$ to obtain $W_{\text{out}} = (10 - 4 + 0)/2 + 1 = 4$ (though the latter is very uncommon and thus not allowed in our setting; we only allow $F \in \{3, 5\}$, as described in Appendix E.1). While this constraint is not trivially fulfilled (which can be verified by manually trying different configurations of W_{in}, F, S, P), it is also not too challenging to find valid configurations.

Note that this constraint is required to be fulfilled for every convolutional layer; we thus obtain the following two constraints in our specific two-layer setting, where $W_{\text{in}} = 28$ (as

MNIST and FashionMNIST images are of shape 28×28):

$$W_{\text{out}1}^e = (28 - F_1^e + P_1^e)/S_1^e + 1 \in \mathbb{N}, \quad (4)$$

$$W_{\text{out}2}^e = (W_{\text{out}1}^e - F_2^e + P_2^e)/S_2^e + 1 \in \mathbb{N}. \quad (5)$$

where the subscripts in $\{1, 2\}$ denote the index of the convolutional layer.

Finally, observe that the constraints in Eq. (4) and Eq. (5) are, respectively, linear and quadratic in the discrete variables $F_1^e, F_2^e, P_1^e, P_2^e, S_1^e, S_2^e$, and can thus be readily incorporated into the integer programming solver (e.g. Gurobi [Optimization, 2014] or CPLEX [IBM, 2009]) we employ as a subroutine within our acquisition function optimization strategy.

Decoder constraints. While the constraints on the decoder architecture are similar in nature to those for the encoder, they are significantly more difficult to fulfill, which we will now illustrate.

In particular, we need to ensure that the decoder produces images of shape 28×28 . By inverting the formula in Eq. (3), we see that for a deconvolutional layer (which intuitively implements an inversion of the convolution operation), the output image size W_{out} can be computed as

$$W_{\text{out}}^d = (W_{\text{in}}^d - 1) \times S^d + F^d - 2P^d + O^d \quad (6)$$

where superscripts d are used to make clear that we are considering the decoder, and where O is an additional output padding parameter which can be used to adjust the shape of the output image⁶. Note that we now have a factor of $2P$ in Eq. (6) instead of P (as for the encoder, i.e. in Eq. (3)), since we only consider symmetric padding for the decoder, while we allow for asymmetric padding for the encoder (to make it easier to fulfill the integrality constraints for the encoder due to an increased number of valid configurations). The output padding parameter O is required since the mapping from W_{in}^e to W_{out}^e in a convolutional layer (i.e. in the encoder) is not bijective: there are different combinations of W_{in}^e, F, S, P that result in the same W_{out}^e (which can be easily verified). Thus, given an output size W_{out}^e (now serving as the input size W_{in}^d of the deconvolutional layer), there is no unique corresponding input size W_{in}^e (now serving as the output size W_{out}^d of the deconvolutional layer). The output padding parameter O can thus be used to disambiguate this relation. Note that W_{out}^d in Eq. (6) is always integral, so there are no integrality constraints involved here, in contrast to the encoder.

In the context of our decoder model, i.e. with up to two deconvolutional layers, and with a required output image size of 28, we thus obtain the following constraints:

$$W_{\text{out}}^d = (W_{\text{in}}^d - 1) \times S_1^d + F_1^d - 2P_1^d + O_1^d, \quad (7)$$

$$28 = (W_{\text{out}}^d - 1) \times S_2^d + F_2^d - 2P_2^d + O_2^d, \quad (8)$$

i.e. we need to choose the parameters $F_1^d, F_2^d, P_1^d, P_2^d, S_1^d, S_2^d, O_1^d, O_2^d$ such that the output size is 28, which is challenging, as only a small number of parameter configurations fulfill this property. While this problem is already challenging when assuming a given fixed

⁶See e.g. <https://pytorch.org/docs/stable/nn.html#convtranspose2d> for a description of the output padding in the context of the PyTorch library we use.

input image shape W_{in}^d , in our setting it is more difficult, as W_{in}^d has to be of a suitable size as well. Note that W_{in}^d is determined by the size of the fully-connected layer preceding the first deconvolutional layer, which yields an additional challenge: the size of the last fully-connected layer has to be set such that it can be resized to an image of shape $C_1^d \times W_{\text{in}}^d \times W_{\text{in}}^d$ (i.e., such that it can be fed into a deconvolutional layer), where C_1^d denotes the number of channels of the first deconvolutional layer of the decoder. As the resulting problem would be too challenging for any algorithm to produce a valid solution in a reasonable amount of time, we simplify it slightly by only treating C_1^d as a design parameter (as described in Appendix E.1), but keeping $W_{\text{in}}^d = 7$ fixed. The value 7 is chosen since $16 \times 7 \times 7 = 784$, i.e., when setting $C_1^d = 16$, the last fully-connected layer has the correct output shape (since $28 \times 28 = 784$ for an MNIST and FashionMNIST image). This way, a valid decoder architecture can be achieved by deactivating all convolutional layers and choosing $C_1^d = 16$, constituting an alternative if fulfilling the decoder constraints in Eq. (7) and Eq. (8) is too challenging for an algorithm.

Finally, the constraints in Eq. (7) and Eq. (8) are, respectively, linear and quadratic in the discrete variables $F_1^d, F_2^d, P_1^d, P_2^d, S_1^d, S_2^d, O_1^d, O_2^d$, which again allows us to incorporate them into our optimization routine.

E.3 Effect of Different Constraint Violation Penalty Values

We now analyze the effect of the constraint violation penalty value on the performance of SMAC, TPE and GPyOpt. Note that random search and MIVABO are not affected by the penalty. We do this analysis to show that the choice of penalty does not qualitatively affect the reported results. In addition to the penalty of 500 nats considered in the experiments in the main paper, we assessed two smaller alternative penalties of 250 nats and 125 nats, respectively. The results in Table 3 show that the performance of the methods improves marginally with decreasing penalty values. This can be intuitively explained by the fact that the smaller the penalty, the smaller the region in hyperparameter space that the penalty discourages from searching. In fact, a large penalty may not only discourage infeasible configurations, but also feasible configurations that lie "close" to the penalized infeasible one (where closeness is defined by the specific surrogate model employed by the method). However, even for the smallest penalty of 125 nats, SMAC, TPE and GPyOpt still perform worse than random search, and thus still significantly worse than MIVABO. Imposing penalties that are significantly smaller than 125 is not sensible, as this will encourage the model-based methods to violate the constraints, and in turn discourage them from ever evaluating a valid configuration (as this would yield a worse score).

Finally, Table 4 shows the number of constraint violations by the different methods, depending on the violation penalty.

E.4 Visualization of Reconstruction Quality

While log-likelihood scores allow for a principled quantitative comparison between different algorithms, they are typically hard to interpret for humans. We thus in Fig. 7 visualize

Table 3: Mean plus/minus one standard deviation of the negative test log-likelihood over 8 random initializations, achieved by the best VAE configuration found by SMAC, TPE and GPyOpt after 16 BO iterations, for constraint violation penalties of 500, 250 and 125 nats. Performance values of MiVABO and random search (which are not affected by the penalty) are included for reference.

Algorithm	Penalty (nats)		
	500	250	125
SMAC	113.0 ± 1.8	112.1 ± 1.8	111.1 ± 1.6
TPE	108.8 ± 1.2	108.1 ± 1.3	108.1 ± 1.3
GPyOpt	108.5 ± 1.1	108.5 ± 0.6	106.5 ± 1.4
RS			106.3 ± 0.9
MiVABO			94.4 ± 0.8

Table 4: Mean plus/minus one standard deviation of the number of constraint violations by SMAC, TPE, GPyOpt and random search within 16 BO iterations over 8 random initializations, for constraint violation penalties of 500, 250 and 125 nats.

Algorithm	Penalty (nats)		
	500	250	125
SMAC	37 ± 21.7	36 ± 21.9	28 ± 11.6
TPE	67 ± 21.3	68 ± 22.2	68 ± 22.2
GPyOpt	36 ± 19.3	32 ± 18.0	27 ± 10.4
Random search	71 ± 25.5	71 ± 25.5	71 ± 25.5

the reconstruction quality achieved by the best VAE configuration found by the different methods after 32 BO iterations. The VAEs were trained for 32 epochs each (as in the BO experiments). The log-likelihood scores seem to be correlated with quality of visual appearance, and the model found by MiVABO thus may be perceived to produce the visually most appealing reconstructions among all models.

F Discussion and Details on Baselines in Empirical Evaluation

We decided to compare against SMAC [Hutter *et al.*, 2011] and TPE [Bergstra *et al.*, 2011], as these are state-of-the-art mixed-variable BO methods. We used their publicly available Python implementations under <https://github.com/automl/SMAC3> (SMAC) and <https://github.com/hyperopt/hyperopt> (TPE). We furthermore compare against the popular popular GPyOpt BO Python package [González, 2016] (<https://github.com/SheffieldML/GPyOpt>) as a reference implementation of a state-of-the-art continuous BO method (which extends to the mixed-variable setting via relaxation and rounding of the discrete variables). We use these Python packages with their respective default settings. Moreover, to isolate the benefit of the model choice from the acquisition function optimization procedure, we consider baselines that, respectively, use the MiVABO and GP models, and optimize the resulting acquisition function using simulated annealing (SA) [Kirkpatrick *et al.*, 1983]. For the baseline that combines a GP with simulated annealing, we use the popular GPy Python package [GPy, since 2012] (which also serves as the GP backend



Figure 7: Visualization of the reconstruction quality of a random subset of (non-binarized) images from the MNIST test set, as achieved by the best VAE model (trained for 32 epochs) found by each method. From left to right: ground truth, MiVABO, random search, GPyOpt, TPE and SMAC. The images are thus ordered (from left to right) by increasing negative test log-likelihood achieved by the VAEs used for reconstruction. Interestingly, the log-likelihood seems to capture quality of visual appearance, as the reconstruction quality may be roughly perceived to decrease from left to right.

of GPyOpt) together with the simulated annealing implementation at <https://github.com/perrygeo/simanneal>. Finally, we compare against random search (using a custom implementation due to its simplicity), which has been shown to be an effective baseline for hyperparameter optimization [Bergstra *et al.*, 2011].

There are several other methods which address problem settings related to the (constrained) mixed-variable paradigm we consider. We here briefly clarify why we decided to not compare against them in our empirical evaluation. Firstly, [Baptista and Poloczek, 2018; Oh *et al.*, 2019; Kim *et al.*, 2019] extend BO to tackle purely discrete/combinatorial problems; these approaches can thus not straightforwardly handle the continuous variables present in mixed-variable problems. [Ru *et al.*, 2019] address BO problems with multiple continuous and *categorical* input variables (i.e. unordered ones), whereas MIVABO includes ordered discrete variables such as integer variables. As pointed out in Section 1, Hyperband [Li *et al.*, 2018] and BOHB [Falkner *et al.*, 2018] are complementary to MIVABO in that they do not propose new mixed-variable methods, but rather extend existing ones (such as random search and TPE) to the multi-fidelity setting; they should thus not be perceived as competing methods. The work of [Garrido-Merchán and Hernández-Lobato, 2018] extends GP-based BO to integer variables, but cannot handle discrete constraints. While several works [Hernández-Lobato *et al.*, 2015a; Gardner *et al.*, 2014; Sui *et al.*, 2015] propose extensions of continuous BO methods to handle unknown constraints, they can neither handle mixed-variable problems nor known (discrete) constraints, and might thus again be viewed as complementary to our approach.

Finally, a recent line of work extends continuous BO methods to general highly structured input spaces such as graphs or images (which also includes mixed discrete-continuous problems), by first training a deep generative model such as a VAE on the input data, and then using standard continuous BO methods in the continuous latent space learned by the VAE [Gómez-Bombarelli *et al.*, 2018]. This so-called *latent space optimization* approach has recently been successfully applied to application domains including automatic chemical design and automatic machine learning [Gómez-Bombarelli *et al.*, 2018; Kusner *et al.*, 2017; Nguyen *et al.*, 2016; Luo *et al.*, 2018; Lu *et al.*, 2018; Jin *et al.*, 2018; Tripp *et al.*, 2020], and might thus be perceived to be a promising method for the mixed-variable hyperparameter tuning tasks we consider in this paper. However, despite these successes, the latent space optimization paradigm is at an early stage and current methods still suffer from critical shortcomings. One of the most severe issues is that the BO procedure tends to progress into regions of the latent space that are too far away from the regions corresponding to the training data, which often results in the BO method suggesting meaningless or even invalid inputs to query (e.g. unreasonable/invalid hyperparameter configurations). Despite recent efforts attempting to mitigate this issue [Kusner *et al.*, 2017; Griffiths and Hernández-Lobato, 2017; Dai *et al.*, 2018; Daxberger and Hernández-Lobato, 2019; Mahmood and Hernández-Lobato, 2019], a robust and principled solution has yet to be found. This issue also reveals that the latent space optimization paradigm makes it difficult to incorporate (discrete) constraints, as the optimization is performed in a learned continuous latent space rather than in the original input space (over which the constraints are defined). As a result, we decided to not compare against latent space optimization methods at this stage, although we point out that this would be an interesting direction for future work.

G Acquisition Function Optimization with Theoretical Guarantees via Dual Decomposition

As an alternative to the alternating optimization scheme proposed in Section 3.3, one can also minimize the acquisition function in Eq. (2) via dual decomposition - a powerful approach based on Lagrangian optimization, which has well-studied theoretical properties and has been successfully used for many different problems [Komodakis *et al.*, 2011; Sontag *et al.*, 2011; Rush and Collins, 2012]. Despite its versatility, the core idea is simple: decompose the initial problem into smaller solvable subproblems and then extract a solution by cleverly combining the solutions from these subproblems [Komodakis *et al.*, 2011]. This requires the following two components: (1) A set of *subproblems* which are defined such that their sum corresponds to the optimization objective, and which can each be optimized globally, and (2) a so-called *master* problem that coordinates the subproblems to find a solution to the original problem. One major advantage of dual decomposition algorithms is that they have well-understood theoretical properties⁷, in particular through connections to linear programming (LP) relaxations. In fact, they enjoy the best theoretical guarantees in terms of convergence properties, when compared to other algorithms solving this problem [Komodakis *et al.*, 2011]. These theoretical properties further facilitate the convergence analysis of MIVABO outlined in Section 3.5, making dual decomposition algorithms particularly useful for settings where optimization accuracy is of crucial importance.

We now describe how to devise a dual decomposition for our problem, by demonstrating how it can be reformulated in terms of master- and sub-problems (see Appendix H for a detailed derivation). For convenience, let us denote the discrete, continuous and mixed parts of Eq. (2) by $f^d(\mathbf{x}^d) = \mathbf{w}^d \top \phi^d(\mathbf{x}^d)$, $f^c(\mathbf{x}^c) = \mathbf{w}^c \top \phi^c(\mathbf{x}^c)$ and $f^m(\mathbf{x}^d, \mathbf{x}^c) = \mathbf{w}^m \top \phi^m(\mathbf{x}^d, \mathbf{x}^c)$, respectively, thus resulting in the representation $f(\mathbf{x}) = f^d(\mathbf{x}^d) + f^c(\mathbf{x}^c) + f^m(\mathbf{x}^d, \mathbf{x}^c)$. First, we note that the discrete $f^d(\mathbf{x}^d)$ and continuous $f^c(\mathbf{x}^c)$ parts of Eq. (2) already represent easy to solve subproblems (as we assume to have access to an optimization oracle). It thus remains to discuss the mixed part $f^m(\mathbf{x}^d, \mathbf{x}^c)$. As f^m is generally difficult to optimize directly, we assume that it decomposes into a sum $f^m(\mathbf{x}) = \sum_{k=1}^{|F|} f_k^m(\mathbf{x}_k^d, \mathbf{x}_k^c)$ of so-called *factors* $f_k^m : \mathcal{X}_k^d \times \mathcal{X}_k^c \rightarrow \mathbb{R}$, where $\mathbf{x}_k^d \in \mathcal{X}_k^d$ and $\mathbf{x}_k^c \in \mathcal{X}_k^c$ respectively denote subvectors of \mathbf{x}^d and \mathbf{x}^c from the (typically low-dimensional) subspaces $\mathcal{X}_k^d \subseteq \mathcal{X}^d$ and $\mathcal{X}_k^c \subseteq \mathcal{X}^c$. Here, F denotes a set of subsets $k \in F$ of the variables. Given this formulation, the initial problem then reduces⁸ to the minimization of the dual function $L(\boldsymbol{\lambda})$ w.r.t. Lagrange multipliers $\boldsymbol{\lambda}$, i.e., the master problem $\min_{\boldsymbol{\lambda}} L(\boldsymbol{\lambda})$, with dual function $L(\boldsymbol{\lambda}) = \max_{\mathbf{x}^d} \{f^d(\mathbf{x}^d) + \sum_{k \in F} \boldsymbol{\lambda}_k^d \mathbf{x}_k^d\} + \max_{\mathbf{x}^c} \{f^c(\mathbf{x}^c) + \sum_{k \in F} \boldsymbol{\lambda}_k^c \mathbf{x}_k^c\} + \sum_{k \in F} \max_{\mathbf{x}_k^d, \mathbf{x}_k^c} \{f_k^m(\mathbf{x}_k^d, \mathbf{x}_k^c) - \boldsymbol{\lambda}_k^d \mathbf{x}_k^d -$

⁷For details, we refer the interested reader to [Komodakis *et al.*, 2011; Sontag *et al.*, 2011; Rush and Collins, 2012]

⁸Refer to Appendix H for a detailed derivation.

$\lambda_k^c \mathbf{x}_k^c$. Here, the master problem coordinates the $2 + |F|$ maximization subproblems, where $\mathbf{x}_{|k}^d$ and $\mathbf{x}_{|k}^c$ respectively denote the subvectors of \mathbf{x}^d and \mathbf{x}^c containing only the variables of factor $k \in F$, λ_k^d and λ_k^c are their corresponding Lagrange multipliers. Intuitively, by updating the dual variables λ , the master problem ensures agreement on the involved variables between the discrete and continuous subproblems and the mixed factors. Importantly, the dual function $L(\lambda)$ only involves independent maximization over local assignments of \mathbf{x}^d , \mathbf{x}^c and \mathbf{x}_k^d , \mathbf{x}_k^c , which are assumed to be tractable. There are two main classes of algorithms used for the maximization, namely subgradient methods and block coordinate descent [Sontag *et al.*, 2011].

H Derivation of Dual Decomposition

One interesting interpretation of our acquisition function optimization problem as defined in Section 3.3 is as *maximum a posteriori* (MAP) inference in the undirected graphical model, or Markov random field (MRF) [Koller *et al.*, 2009], induced by the dependency graph of the involved variables (i.e. the graph in which vertices correspond to variables, and edges appear between variables that interact in some way). We take this perspective and devise a dual decomposition to tackle the MAP estimation problem induced by our particular setting (i.e., interpreting our acquisition function as the energy function of the graphical model), following the formulation of [Sontag *et al.*, 2011].⁹

Consider a graphical model on the vertex set $\mathcal{V} = V_d \cup V_c$, where the vertices $V_d = \{1, \dots, D_d\}$ and $V_c = \{D_d + 1, \dots, D_d + D_c\}$ correspond to the discrete and continuous variables $\mathbf{x}^d \in \mathcal{X}^d$ and $\mathbf{x}^c \in \mathcal{X}^c$, respectively. Furthermore, consider a set F of subsets of both discrete and continuous variables/vertices, i.e., $\forall f \in F : f = (f^d \cup f^c) \subseteq V, \emptyset \neq f^d \subseteq V_d, \emptyset \neq f^c \subseteq V_c$, where each subset corresponds to the domain of one of the factors.

Now assume that we are given the following functions on these factors as well as on all discrete/continuous variables:

- A factor $\theta^d(\mathbf{x}^d), \theta^d : \mathcal{X}^d \rightarrow \mathbb{R}$ on all discrete variables
- A factor $\theta^c(\mathbf{x}^c), \theta^c : \mathcal{X}^c \rightarrow \mathbb{R}$ on all continuous variables
- $|F|$ mixed factors $\theta_f^m(\mathbf{x}_f^d, \mathbf{x}_f^c), \theta_f^m : \mathcal{X}_f^d \times \mathcal{X}_f^c \rightarrow \mathbb{R}$ on subsets $f \in F$ of both discrete and continuous variables, where $\mathbf{x}_f^d \in \mathcal{X}_f^d$ and $\mathbf{x}_f^c \in \mathcal{X}_f^c$ respectively denote subvectors of \mathbf{x}^d and \mathbf{x}^c from the (typically low-dimensional) subspaces $\mathcal{X}_f^d \subseteq \mathcal{X}^d$ and $\mathcal{X}_f^c \subseteq \mathcal{X}^c$, indexed by the vertices contained in f

The goal of our MAP problem is to find an assignment to all variables \mathbf{x}^d and \mathbf{x}^c which maximizes the sum of the factors:

$$\text{MAP}(\theta) = \max_{\mathbf{x}} \left\{ \theta^d(\mathbf{x}^d) + \theta^c(\mathbf{x}^c) + \sum_{f \in F} \theta_f^m(\mathbf{x}_f^d, \mathbf{x}_f^c) \right\} \quad (9)$$

⁹In accordance with the notation in [Sontag *et al.*, 2011], we will here denote the factors by θ instead of f (i.e., in contrast to the main text).

We now slightly reformulate this problem by duplicating the variables x_i^d and x_j^c , once for each mixed factor $\theta_f^m(\mathbf{x}_f^d, \mathbf{x}_f^c)$, and then enforce that these variables are equal to the ones appearing in the factors $\theta^d(\mathbf{x}^d)$ and $\theta^c(\mathbf{x}^c)$, respectively. Let x_i^{df} and x_j^{cf} respectively denote the copy of x_i^d and x_j^c used by factor f . Moreover, denote by $\mathbf{x}_f^{df} = \{x_i^{df}\}_{i \in f^d}$ and $\mathbf{x}_f^{cf} = \{x_j^{cf}\}_{j \in f^c}$ the set of variables used by factor f , and by $\mathbf{x}^F = \{\mathbf{x}_f^{df}, \mathbf{x}_f^{cf}\}_{f \in F}$ the set of all variable copies. We then get the equivalent (but now constrained) optimization problem

$$\max_{\mathbf{x}, \mathbf{x}^F} \left\{ \theta^d(\mathbf{x}^d) + \theta^c(\mathbf{x}^c) + \sum_{f \in F} \theta_f^m(\mathbf{x}_f^{df}, \mathbf{x}_f^{cf}) \right\} \quad (10)$$

$$\begin{aligned} \text{s.t. } & x_i^{df} = x_i^d, \quad \forall f \in F, i \in f^d \\ & x_j^{cf} = x_j^c, \quad \forall f \in F, j \in f^c \end{aligned}$$

To remove the coupling constraints, [Sontag *et al.*, 2011] now propose to use the technique of *Lagrangian relaxation* and introduce a Lagrange multiplier / dual variable $\lambda_{fi}(x_i)$ for every choice of $f \in F, i \in f$ and x_i (i.e. for every factor, for every variable in that factor, and for every value of that variable). These multipliers may then be interpreted as the *message* that factor f sends to variable i about its state x_i .

While this works well if all variables are discrete, in our model we also have continuous variables x_j^c , and it is clearly not possible to have a Lagrange multiplier for every possible value of x_j^c . To mitigate this issue, we follow [Komodakis *et al.*, 2011] and instead only introduce a multiplier λ_{fi} for every choice of $f \in F$ and $i \in f$, and model the interaction with the variables as $\lambda_{fi}(x_i) = \lambda_{fi} x_i$ (i.e., the product of a multiplier λ_{fi} and variable x_i). Observe that since our goal is to relax the coupling constraints, it is sufficient to introduce one multiplier per constraint. Since we have a constraint for every factor $f \in F$ and every discrete variable $i \in f^d$ and continuous variable $j \in f^c$ in that factor, our approach is clearly viable.

Note that in contrast to [Komodakis *et al.*, 2011], that introduces a set of multipliers for *every* factor / subgraph, we only introduce multipliers for the *mixed* factors $f \in F$. This is because in contrast to [Komodakis *et al.*, 2011], we do not introduce a full set of variable copies for *every* factor and then couple them to another global set of "original" variables, but we instead only introduce variable copies for the *mixed* factors and couple them to the variables appearing in the *discrete and continuous* factors, which we assume to be the "original" variables instead. This essentially is the same approach used in [Sontag *et al.*, 2011], with the difference that [Sontag *et al.*, 2011] introduce a singleton factor for each variable (i.e., a factor which depends only on a single variable), which they consider to be the "original" variable. They then simply couple the variable copies appearing in the *higher-order* factors to the "original" variables appearing in the *singleton* factors. In contrast, in our formulation we don't introduce singleton factors to model the "original" variables, but instead use the *fully discrete and continuous* factors for this purpose, which clearly works equally well. Note that as a result of this modeling choice, our optimization problem will be unconstrained,

regardless of the number of factors, similar as in [Sontag *et al.*, 2011]. In contrast, [Komodakis *et al.*, 2011] end up with constraints enforcing that some of the dual variables sum to zero, since they are optimizing out the global set of "original" variables from their objective, while we keep the set of "original" variables within our discrete and continuous factors. For this reason, we will in contrast to [Komodakis *et al.*, 2011] later not require a projection step within the subgradient method used to optimize the dual; this is to be detailed further below.

For clarity, we treat discrete and continuous variables distinctly and for factor $f \in F$ denote λ_{fi}^d and λ_{fj}^c respectively for the Lagrange multipliers corresponding to its discrete variables $i \in f^d$ (or rather, the constraints $x_i^{df} = x_i^d$) and its continuous variables $j \in f^c$ (or rather, the constraints $x_j^{cf} = x_j^c$). For every factor $f \in F$, we furthermore aggregate its multipliers into the vectors $\boldsymbol{\lambda}_f^d = \{\lambda_{fi}^d\}_{i \in f^d} \in \mathbb{R}^{|\mathcal{X}_f^d|}$ and $\boldsymbol{\lambda}_f^c = \{\lambda_{fj}^c\}_{j \in f^c} \in \mathbb{R}^{|\mathcal{X}_f^c|}$. The set of all Lagrange multipliers is thus $\boldsymbol{\lambda} = \{\lambda_{fi}^d : f \in F, i \in f^d\} \cup \{\lambda_{fj}^c : f \in F, j \in f^c\} = \{\boldsymbol{\lambda}_f^d, \boldsymbol{\lambda}_f^c\}_{f \in F}$. We then define the Lagrangian

$$\begin{aligned} L(\boldsymbol{\lambda}, \mathbf{x}, \mathbf{x}^F) &= \theta^d(\mathbf{x}^d) + \theta^c(\mathbf{x}^c) + \sum_{f \in F} \theta_f^m(\mathbf{x}_f^{df}, \mathbf{x}_f^{cf}) \\ &+ \sum_{f \in F} \sum_{i \in f^d} \lambda_{fi}^d (x_i^d - x_i^{df}) + \sum_{f \in F} \sum_{j \in f^c} \lambda_{fj}^c (x_j^c - x_j^{cf}) \\ &= \left(\theta^d(\mathbf{x}^d) + \sum_{f \in F} \sum_{i \in f^d} \lambda_{fi}^d x_i^d \right) \\ &+ \left(\theta^c(\mathbf{x}^c) + \sum_{f \in F} \sum_{j \in f^c} \lambda_{fj}^c x_j^c \right) \\ &+ \sum_{f \in F} \left(\theta_f^m(\mathbf{x}_f^{df}, \mathbf{x}_f^{cf}) - \sum_{i \in f^d} \lambda_{fi}^d x_i^{df} - \sum_{j \in f^c} \lambda_{fj}^c x_j^{cf} \right). \end{aligned}$$

This results in the following optimization problem:

$$\begin{aligned} &\max_{\boldsymbol{\lambda}, \mathbf{x}^F} L(\boldsymbol{\lambda}, \mathbf{x}, \mathbf{x}^F) \quad (11) \\ \text{s.t. } &x_i^{df} = x_i^d, \quad \forall f \in F, i \in f^d \\ &x_j^{cf} = x_j^c, \quad \forall f \in F, j \in f^c \end{aligned}$$

Note that the problem in Eq. (11) is still equivalent to our (hard) original problem in Eq. (9) for any assignment of $\boldsymbol{\lambda}$, since the Lagrange multipliers cancel out if all coupling constraints are fulfilled.

To obtain a tractable problem, we thus simply omit the coupling constraints in Eq. (11) and define the dual function $L(\boldsymbol{\lambda})$

as

$$\begin{aligned} L(\boldsymbol{\lambda}) &= \max_{\mathbf{x}, \mathbf{x}^F} L(\boldsymbol{\lambda}, \mathbf{x}, \mathbf{x}^F) \\ &= \max_{\mathbf{x}^d} \left(\theta^d(\mathbf{x}^d) + \sum_{f \in F} \sum_{i \in f^d} \lambda_{fi}^d x_i^d \right) \\ &+ \max_{\mathbf{x}^c} \left(\theta^c(\mathbf{x}^c) + \sum_{f \in F} \sum_{j \in f^c} \lambda_{fj}^c x_j^c \right) \\ &+ \sum_{f \in F} \max_{\mathbf{x}_f^{df}, \mathbf{x}_f^{cf}} \left(\theta_f^m(\mathbf{x}_f^{df}, \mathbf{x}_f^{cf}) - \sum_{i \in f^d} \lambda_{fi}^d x_i^{df} - \sum_{j \in f^c} \lambda_{fj}^c x_j^{cf} \right) \end{aligned}$$

Note that the maximizations are now fully independent, such that we can (without introducing any ambiguity) simplify the notation for the variables involved in the mixed terms to denote \mathbf{x}_f^d and \mathbf{x}_f^c instead of \mathbf{x}_f^{df} and \mathbf{x}_f^{cf} , respectively¹⁰, resulting in the slightly simpler dual formulation

$$\begin{aligned} L(\boldsymbol{\lambda}) &= \max_{\mathbf{x}^d} \left(\theta^d(\mathbf{x}^d) + \sum_{f \in F} \sum_{i \in f^d} \lambda_{fi}^d x_i^d \right) \\ &+ \max_{\mathbf{x}^c} \left(\theta^c(\mathbf{x}^c) + \sum_{f \in F} \sum_{j \in f^c} \lambda_{fj}^c x_j^c \right) \\ &+ \sum_{f \in F} \max_{\mathbf{x}_f^d, \mathbf{x}_f^c} \left(\theta_f^m(\mathbf{x}_f^d, \mathbf{x}_f^c) - \sum_{i \in f^d} \lambda_{fi}^d x_i^d - \sum_{j \in f^c} \lambda_{fj}^c x_j^c \right) \end{aligned}$$

Let $\mathbf{x}_{|f}^d \in \mathcal{X}_f^d$ and $\mathbf{x}_{|f}^c \in \mathcal{X}_f^c$ respectively denote the subvectors of \mathbf{x}^d and \mathbf{x}^c containing only the variables of factor f . The shorthands (or *reparameterizations* [Sontag *et al.*, 2011])

$$\begin{aligned} \bar{\theta}_d^\lambda(\mathbf{x}^d) &= \theta^d(\mathbf{x}^d) + \sum_{f \in F} \sum_{i \in f^d} \lambda_{fi}^d x_i^d \\ &= \theta^d(\mathbf{x}^d) + \sum_{f \in F} \boldsymbol{\lambda}_f^d \mathbf{x}_{|f}^d \quad (12) \end{aligned}$$

$$\begin{aligned} \bar{\theta}_c^\lambda(\mathbf{x}^c) &= \theta^c(\mathbf{x}^c) + \sum_{f \in F} \sum_{j \in f^c} \lambda_{fj}^c x_j^c \\ &= \theta^c(\mathbf{x}^c) + \sum_{f \in F} \boldsymbol{\lambda}_f^c \mathbf{x}_{|f}^c \quad (13) \end{aligned}$$

$$\begin{aligned} \bar{\theta}_f^\lambda(\mathbf{x}_f^d, \mathbf{x}_f^c) &= \theta_f^m(\mathbf{x}_f^d, \mathbf{x}_f^c) - \sum_{i \in f^d} \lambda_{fi}^d x_i^d - \sum_{j \in f^c} \lambda_{fj}^c x_j^c \\ &= \theta_f^m(\mathbf{x}_f^d, \mathbf{x}_f^c) - \boldsymbol{\lambda}_f^d \mathbf{x}_f^d - \boldsymbol{\lambda}_f^c \mathbf{x}_f^c \quad (14) \end{aligned}$$

further simplify the dual function $L(\boldsymbol{\lambda})$ to

$$L(\boldsymbol{\lambda}) = \max_{\mathbf{x}^d} \bar{\theta}_d^\lambda(\mathbf{x}^d) + \max_{\mathbf{x}^c} \bar{\theta}_c^\lambda(\mathbf{x}^c) + \sum_{f \in F} \max_{\mathbf{x}_f^d, \mathbf{x}_f^c} \bar{\theta}_f^\lambda(\mathbf{x}_f^d, \mathbf{x}_f^c). \quad (15)$$

¹⁰I.e., we replace all variable copies $\mathbf{x}_f^{df}, \mathbf{x}_f^{cf}$ in the mixed terms by the "original" variables $\mathbf{x}_f^d, \mathbf{x}_f^c$.

First, observe that since we maximize over \mathbf{x} and \mathbf{x}^F , the dual function $L(\boldsymbol{\lambda})$ is a function of just the Lagrange multipliers $\boldsymbol{\lambda}$. Note that since $L(\boldsymbol{\lambda})$ maximizes over a larger space (since instead of forcing that there must be one global assignment maximizing the objective, we allow the discrete/continuous potentials to be maximized independently of the mixed potentials, meaning that \mathbf{x} may not coincide with \mathbf{x}^F), we have for all $\boldsymbol{\lambda}$ that

$$\text{MAP}(\boldsymbol{\theta}) \leq L(\boldsymbol{\lambda}). \quad (16)$$

The *dual problem* now is to find the tightest upper bound by optimizing the Lagrange multipliers, i.e.

$$\min_{\boldsymbol{\lambda}} L(\boldsymbol{\lambda}) \quad (17)$$

We also call the dual problem in Eq. (17) the *master problem*, which coordinates the $2 + |F|$ *slave problems* (i.e., one for each factor)

$$s^d(\boldsymbol{\lambda}) = \max_{\mathbf{x}^d} \bar{\theta}_d^\lambda(\mathbf{x}^d) \quad (18a)$$

$$s^c(\boldsymbol{\lambda}) = \max_{\mathbf{x}^c} \bar{\theta}_c^\lambda(\mathbf{x}^c) \quad (18b)$$

$$s^f(\boldsymbol{\lambda}) = \max_{\mathbf{x}_f^d, \mathbf{x}_f^c} \bar{\theta}_f^\lambda(\mathbf{x}_f^d, \mathbf{x}_f^c), \quad \forall f \in F. \quad (18c)$$

where we refer to s^d , s^c and s^f as the discrete slave, the continuous slave, and the mixed slaves, respectively. Using the notation in Eqs. (18a)-(18c), the dual function further simplifies to

$$L(\boldsymbol{\lambda}) = s^d(\boldsymbol{\lambda}) + s^c(\boldsymbol{\lambda}) + \sum_{f \in F} s^f(\boldsymbol{\lambda}). \quad (19)$$

Intuitively, the goal of Eq. (17) is as follows: The master problem wants the discrete/continuous slaves to agree with the mixed slaves/factors in which the corresponding discrete/continuous variables appear, and conversely, it wants the mixed slaves to agree with the slaves/factors of the discrete/continuous variables in its scope. The master problem will thus incentivize the discrete/continuous slaves and the mixed slaves to agree with each other, which is done by updating the dual variables $\boldsymbol{\lambda}$ accordingly.

The key property of the function $L(\boldsymbol{\lambda})$ is that it only involves maximization over local assignments of \mathbf{x}^d , \mathbf{x}^c and \mathbf{x}_f^d , \mathbf{x}_f^c , which are tasks we assume to be tractable. The dual thus decouples the original problem, resulting in a problem that can be optimized using local operations. Algorithms that minimize the approximate objective $L(\boldsymbol{\lambda})$ use local updates where each iteration of the algorithms repeatedly finds a maximizing assignment for the subproblems individually, using these to update the dual variables $\boldsymbol{\lambda}$ that glue the subproblems together. There are two main classes of algorithms of this kind, one based on a subgradient method and another based on block coordinate descent [Sontag *et al.*, 2011].

References

[Baptista and Poloczek, 2018] Ricardo Baptista and Matthias Poloczek. Bayesian optimization of combinatorial structures. In *ICML*, 2018.

[Bergstra *et al.*, 2011] James S Bergstra, Rémi Bardenet, Yoshua Bengio, and Balázs Kégl. Algorithms for hyperparameter optimization. In *NIPS*, 2011.

[Bishop, 2006] Christopher M Bishop. *Pattern recognition and machine learning*. Springer, 2006.

[Dai *et al.*, 2018] Hanjun Dai, Yingtao Tian, Bo Dai, Steven Skiena, and Le Song. Syntax-directed variational autoencoder for structured data. *arXiv preprint arXiv:1802.08786*, 2018.

[Daxberger and Hernández-Lobato, 2019] Erik Daxberger and José Miguel Hernández-Lobato. Bayesian variational autoencoders for unsupervised out-of-distribution detection. *arXiv preprint arXiv:1912.05651*, 2019.

[Falkner *et al.*, 2018] Stefan Falkner, Aaron Klein, and Frank Hutter. BOHB: Robust and efficient hyperparameter optimization at scale. In *ICML*, 2018.

[Gardner *et al.*, 2014] Jacob R. Gardner, Matt J. Kusner, Zhixiang Xu, Kilian Q. Weinberger, and John P. Cunningham. Bayesian optimization with inequality constraints. In *ICML*, 2014.

[Garrido-Merchán and Hernández-Lobato, 2018] Eduardo C Garrido-Merchán and Daniel Hernández-Lobato. Dealing with categorical and integer-valued variables in bayesian optimization with gaussian processes. *CoRR*, 2018.

[Gómez-Bombarelli *et al.*, 2018] Rafael Gómez-Bombarelli, Jennifer N Wei, David Duvenaud, José Miguel Hernández-Lobato, Benjamín Sánchez-Lengeling, Dennis Sheberla, Jorge Aguilera-Iparraguirre, Timothy D Hirzel, Ryan P Adams, and Alán Aspuru-Guzik. Automatic chemical design using a data-driven continuous representation of molecules. *ACS central science*, 4(2):268–276, 2018.

[González, 2016] J González. GPpyOpt: A Bayesian optimization framework in Python, 2016.

[GPpy, since 2012] GPpy. GPpy: A gaussian process framework in python. <http://github.com/SheffieldML/GPy>, since 2012.

[Griffiths and Hernández-Lobato, 2017] Ryan-Rhys Griffiths and José Miguel Hernández-Lobato. Constrained bayesian optimization for automatic chemical design. *arXiv preprint arXiv:1709.05501*, 2017.

[Hernández-Lobato *et al.*, 2013] Daniel Hernández-Lobato, José Miguel Hernández-Lobato, and Pierre Dupont. Generalized spike-and-slab priors for bayesian group feature selection using expectation propagation. *The Journal of Machine Learning Research*, 14(1):1891–1945, 2013.

[Hernández-Lobato *et al.*, 2015a] José Miguel Hernández-Lobato, Michael A Gelbart, Matthew W Hoffman, Ryan P Adams, and Zoubin Ghahramani. Predictive entropy search for bayesian optimization with unknown constraints. *JMLR*, 2015.

[Hernández-Lobato *et al.*, 2015b] José Miguel Hernández-Lobato, Daniel Hernández-Lobato, and Alberto Suárez. Expectation propagation in linear regression models with

- spike-and-slab priors. *Machine Learning*, 99(3):437–487, 2015.
- [Hutter *et al.*, 2011] Frank Hutter, Holger H Hoos, and Kevin Leyton-Brown. Sequential model-based optimization for general algorithm configuration. In *LION*, 2011.
- [IBM, 2009] IBM. User’s manual for CPLEX. *International Business Machines Corporation*, 46(53):157, 2009.
- [Jin *et al.*, 2018] Wengong Jin, Regina Barzilay, and Tommi Jaakkola. Junction tree variational autoencoder for molecular graph generation. *arXiv preprint arXiv:1802.04364*, 2018.
- [Kim *et al.*, 2019] Jungtaek Kim, Michael McCourt, Tackgeun You, Saehoon Kim, and Seungjin Choi. Bayesian optimization over sets. *arXiv preprint arXiv:1905.09780*, 2019.
- [Kirkpatrick *et al.*, 1983] Scott Kirkpatrick, C Daniel Gelatt, and Mario P Vecchi. Optimization by simulated annealing. *science*, 220(4598):671–680, 1983.
- [Koller *et al.*, 2009] Daphne Koller, Nir Friedman, and Francis Bach. *Probabilistic graphical models: principles and techniques*. MIT press, 2009.
- [Komodakis *et al.*, 2011] Nikos Komodakis, Nikos Paragios, and Georgios Tziritas. MRF energy minimization and beyond via dual decomposition. *IEEE transactions on pattern analysis and machine intelligence*, 2011.
- [Kusner *et al.*, 2017] Matt J Kusner, Brooks Paige, and José Miguel Hernández-Lobato. Grammar variational autoencoder. In *Proceedings of the 34th International Conference on Machine Learning-Volume 70*, pages 1945–1954. JMLR. org, 2017.
- [Li *et al.*, 2018] Lisha Li, Kevin Jamieson, Giulia DeSalvo, Afshin Rostamizadeh, and Ameet Talwalkar. Hyperband: A novel bandit-based approach to hyperparameter optimization. *JMLR*, 2018.
- [Lu *et al.*, 2018] Xiaoyu Lu, Javier Gonzalez, Zhenwen Dai, and Neil Lawrence. Structured variationally auto-encoded optimization. In *International Conference on Machine Learning*, pages 3273–3281, 2018.
- [Luo *et al.*, 2018] Renqian Luo, Fei Tian, Tao Qin, Enhong Chen, and Tie-Yan Liu. Neural architecture optimization. In *Advances in Neural Information Processing Systems*, pages 7827–7838, 2018.
- [Mahmood and Hernández-Lobato, 2019] Omar Mahmood and José Miguel Hernández-Lobato. A cold approach to generating optimal samples. *arXiv preprint arXiv:1905.09885*, 2019.
- [Minka, 2001] Thomas P Minka. Expectation propagation for approximate Bayesian inference. In *UAI*, pages 362–369, 2001.
- [Nguyen *et al.*, 2016] Anh Nguyen, Alexey Dosovitskiy, Jason Yosinski, Thomas Brox, and Jeff Clune. Synthesizing the preferred inputs for neurons in neural networks via deep generator networks. In *Advances in neural information processing systems*, pages 3387–3395, 2016.
- [Nickisch, 2012] Hannes Nickisch. glm-ie: generalised linear models inference & estimation toolbox. *Journal of Machine Learning Research*, 13(May):1699–1703, 2012.
- [Oh *et al.*, 2019] Changyong Oh, Jakub M. Tomczak, Efstratios Gavves, and Max Welling. Combinatorial bayesian optimization using graph representations. *NeurIPS*, 2019.
- [Optimization, 2014] Gurobi Optimization. Gurobi optimizer reference manual. <http://www.gurobi.com>, 2014.
- [Ru *et al.*, 2019] Binxin Ru, Ahsan S Alvi, Vu Nguyen, Michael A Osborne, and Stephen J Roberts. Bayesian optimisation over multiple continuous and categorical inputs. *arXiv preprint arXiv:1906.08878*, 2019.
- [Rush and Collins, 2012] Alexander M Rush and MJ Collins. A tutorial on dual decomposition and Lagrangian relaxation for inference in natural language processing. *Journal of Artificial Intelligence Research*, 45:305–362, 2012.
- [Seeger and Nickisch, 2008] Matthias W Seeger and Hannes Nickisch. Compressed sensing and bayesian experimental design. In *International Conference on Machine Learning (ICML)*. ACM, 2008.
- [Seeger and Nickisch, 2011] Matthias W Seeger and Hannes Nickisch. Large scale Bayesian inference and experimental design for sparse linear models. *SIAM Journal on Imaging Sciences*, 4(1):166–199, 2011.
- [Seeger, 2008] Matthias W Seeger. Bayesian inference and optimal design for the sparse linear model. *Journal of Machine Learning Research*, 9(Apr):759–813, 2008.
- [Sontag *et al.*, 2011] David Sontag, Amir Globerson, and Tommi Jaakkola. Introduction to dual composition for inference. In *Optimization for Machine Learning*. 2011.
- [Sui *et al.*, 2015] Yanan Sui, Alkis Gotovos, Joel Burdick, and Andreas Krause. Safe exploration for optimization with gaussian processes. In *ICML*, 2015.
- [Tripp *et al.*, 2020] Austin Tripp, Erik Daxberger, and José Miguel Hernández-Lobato. Sample-efficient optimization in the latent space of deep generative models via weighted retraining. *arXiv preprint arXiv:2006.09191*, 2020.
- [Wainwright *et al.*, 2008] Martin J Wainwright, Michael I Jordan, et al. Graphical models, exponential families, and variational inference. *Foundations and Trends® in Machine Learning*, 1(1–2):1–305, 2008.